

## *Pbx3* is required for normal locomotion and dorsal horn development

Catherine A. Rottkamp, Katherine J. Lobur, Cynthia L. Wladyka,  
Amy K. Lucky, Stephen O’Gorman \*

Department of Neurosciences, Rm E640, Case School of Medicine, Cleveland, OH 44106, USA

Received for publication 17 April 2007; revised 27 September 2007; accepted 25 October 2007

Available online 12 November 2007

### Abstract

The transcription cofactor Pbx3 is critical for the function of hindbrain circuits controlling respiration in mammals, but the perinatal lethality caused by constitutively null mutations has hampered investigation of other roles it may play in neural development and function. Here we report that the conditional loss of *Pbx3* function in most tissues caudal to the hindbrain resulted in progressive deficits of posture, locomotion, and sensation that became apparent during adolescence. In adult mutants, the size of the dorsal horn of the spinal cord and the numbers of calbindin-, PKC- $\gamma$ , and calretinin-expressing neurons in laminae I–III were markedly reduced, but the ventral cord and peripheral nervous system appeared normal. In the embryonic dorsal horn, Pbx3 expression was restricted to a subset of glutamatergic neurons, but its absence did not affect the initial balance of excitatory and inhibitory interneuron phenotypes. By embryonic day 15 a subset of Meis(+) glutamatergic neurons assumed abnormally superficial positions and the number of calbindin(+) neurons was increased three-fold in the mutants. Loss of *Pbx3* function thus leads to the incorrect specification of some glutamatergic neurons in the dorsal horn and alters the integration of peripheral sensation into the spinal circuitry regulating locomotion.

© 2007 Elsevier Inc. All rights reserved.

**Keywords:** Hox genes; Tlx genes; Movement disorder; Spinal cord; Dorsal horn; Lamination; Glutamate; GABA; Meis; Calbindin

### Introduction

*Hox* genes encode homeodomain transcription factors that play an essential, conserved role in patterning the body axis during embryogenesis. In the nervous system, Hox function is important for establishing regional and neuronal identities in the hindbrain and spinal cord. In the hindbrain, Hox proteins help to determine the appropriate specification of motor and sensory neurons (Arenkiel et al., 2003; Gaufo et al., 2004; Goddard et al., 1996; Rijli et al., 1993; Studer et al., 1996). In the spinal cord, Hox gene activity is also critical for the establishment of different classes of motor neurons that are generated at brachial, thoracic and lumbar levels (Carpenter et al., 1997; Dasen et al., 2003, 2005; de la Cruz et al., 1999; Wahba et al., 2001). Relatively little is known about the possible roles played by the Hox gene family in establishing the identities of other classes of spinal neurons.

Many Hox gene functions require the activity of members of the PBC family of TALE homeodomain transcriptional cofactors (Mann and Chan, 1996; Ryoo et al., 1999). This family includes Extradenticle (Exd) in *Drosophila* and the Pbx proteins in vertebrates. Cooperative DNA binding by PBC and Hox proteins typically increases the binding specificity and the transcriptional activity of the Hox partner, but more complex interactions have been observed that depend on cellular context (Kobayashi et al., 2003; Pinsonneault et al., 1997; Saleh et al., 2000). In *Drosophila*, the loss of *Exd* function is phenotypically equivalent to the loss of multiple Hox gene activities, even though the Hox proteins are expressed at normal levels in appropriate domains (Peifer and Wieschaus, 1990). In mammals, the several Pbx family members have overlapping expression patterns and show considerable functional redundancy (Moens and Selleri, 2006). Nonetheless, when *Pbx1* function is eliminated in mice the resulting phenotype includes craniofacial, axial, and appendicular skeletal malformations that are also attributes of several Hox null phenotypes (Brendolan et al., 2005; Capellini et al., 2006; Moens and Selleri, 2006; Rhee et al., 2004; Selleri et al., 2001, 2004).

\* Corresponding author. Fax: +1 216 368 4650.

E-mail address: [ogorman@case.edu](mailto:ogorman@case.edu) (S. O’Gorman).

Clear evidence that Pbx proteins influence development of the vertebrate central nervous system comes from studies in both zebrafish and mammals. In zebrafish, the migration of facial motor neurons and the axonal projections of trigeminal motor neurons is abnormal in *Pbx4*<sup>-/-</sup> mutants (Cooper et al., 2003). Suppression of *Pbx2* expression on an *Pbx4*<sup>-/-</sup> background transforms rhombomere 4 and 5 into a rhombomere 1 ground state (Waskiewicz et al., 2001). Recently *Pbx2* and *Pbx4* were implicated in development of rostral structures by cooperating with engrailed proteins (Eng) to maintain the midbrain–hindbrain and diencephalic–mesencephalic boundaries (Erickson et al., 2007).

In mammals, PBC proteins are critical for the proper functioning of hindbrain circuits essential for respiration. *Pbx3*<sup>-/-</sup> mice die at birth from congenital apnea that is thought to be caused by abnormal activity of inspiratory neurons in the ventrolateral medulla (Rhee et al., 2004). It is striking that *Pbx3* null mutations show substantial phenotypic overlap with mutants of the homeodomain transcription factor Tlx3/Rnx, which also display abnormal inspiratory neuron activity in the ventrolateral medulla and C4 motor root (Shirasawa et al., 2000). *Tlx3*, along with *Tlx1*, was subsequently shown to act as a post-mitotic selector gene that promotes glutamatergic over GABAergic cell fates in the dorsal spinal cord (Cheng et al., 2004). The decreased respiratory drive seen in *Tlx3*<sup>-/-</sup> mice can be reversed with GABA antagonists, suggesting that this phenotype reflects a change in the balance of excitation and inhibition in the medulla (Cheng et al., 2004). Pbx3 and Tlx3 proteins bind DNA cooperatively to enhance transcription from Tlx3-responsive elements (Rhee et al., 2004). There is also overlap in the null phenotypes of *Pbx1* and *Tlx1* in that both include asplenia (Dear et al., 1995; Roberts et al., 1994; Selleri et al., 2001). In *Pbx1* null embryos the expression of several genes involved in spleen ontogeny is reduced, and Pbx1 cooperatively binds DNA with Tlx1 to regulate transcription from Tlx1-responsive promoters, including the Tlx1 promoter itself (Brendolan et al., 2005). The similar phenotypes of *Tlx* and PBC null animals and the wide expression of PBC family members in the spinal cord (Di Giacomo et al., 2006; Monica et al., 1991; Rhee et al., 2004; Roberts et al., 1995) suggest that that PBC proteins may cooperate with Tlx3 in the specification of dorsal spinal neurons.

The development of the dorsal spinal cord, which is critical for processing sensory information from the periphery, includes two distinct waves of neurogenesis (Gross et al., 2002; Muller et al., 2002). The early phase (E10–E11.5) generates sensory interneurons that populate deep layers of the dorsal horn. During this phase dorsal neuron precursors can be divided into six classes along the dorsoventral axis by the expression of different combinations of basic helix–loop–helix (bHLH) transcription factors (Casparly and Anderson, 2003; Fitzgerald, 2005). The postmitotic neurons that emerge from these progenitor domains are also divisible into six derivative classes (dII–dI6) of dorsal interneurons expressing different combinations of homeodomain transcription factors (Gross et al., 2002; Muller et al., 2002).

The late phase of neurogenesis (E12–E13.5) gives rise to the neurons that populate the marginal layer (lamina I), the sub-

stantia gelatinosa (lamina II) and the lamina propria (laminae III–IV) of the dorsal horn. In this phase the three most ventral progenitor zones expand dorsally and intermingle to form a single zone (dIL). The dIL precursors generate either GABAergic, inhibitory (dIL<sub>A</sub>) or glutamatergic, excitatory (dIL<sub>B</sub>) interneurons. As mentioned above, *Tlx1* and *Tlx3* are required for the specification of glutamatergic cell fates in the dorsal spinal cord (Cheng et al., 2004). Conversely, *Pf1a* promotes GABAergic fates in part by antagonizing *Tlx1/3* (Glasgow et al., 2005). A number of additional transcription factors (Gsh1/2, Ascl and Lhx1/5) have recently been shown to play roles in either initializing or maintaining this balance (Mizuguchi et al., 2006; Pillai et al., 2007). While much has been learned about the mechanisms that control the balance between excitatory and inhibitory neurons in the dorsal horn, much less is known about how these classes become subdivided into mature functional classes.

In this study, we used conditional genetic ablation to reveal an unanticipated role for *Pbx3* in the development and function of neural circuits controlling movement. Mice in which *Pbx3* function was eliminated in most tissues caudal to the hindbrain lived to adulthood, but displayed progressive movement and sensory disorders associated with neuronal loss and disrupted lamination in the dorsal horn. The specification of dorsal glutamatergic and GABAergic phenotypes initially appeared normal, but some classes of glutamatergic neurons were mispositioned or over-represented. By adolescence, the distribution of CGRP-expressing (CGRP(+)) dorsal root ganglion afferent axons was abnormal, and in adults, the number of dorsal horn neurons was significantly reduced. We hypothesize that *Pbx3* is required for specification of glutamatergic neuron subtypes in the dorsal horn and that the resulting disorganization of dorsal horn lamination creates an imbalance that leads to postnatal neuron loss.

## Materials and methods

### Mouse strains

A lambda clone from a 129SV genomic DNA library containing exon 3 of the *Pbx3* gene and 4 kb of 5' and 10 kb of 3' flanking DNA was obtained from Licia Selleri (Rhee et al., 2004) (Fig. 1). A loxP site was introduced into a *HindIII* site 0.5 kb 5' to exon 3. A neomycin resistance cassette from pMC1-neo (Thomas and Capecchi, 1986) flanked at its 5' end by loxP and FRT sites and at its 3' end by an FRT site was inserted at a *ScaI* site 1.7 kb 3' to the exon. The targeting vector contained 1.7 kb of *Pbx3* sequences 5' to the 5' loxP site and 7.9 kb of *Pbx3* sequences 3' to the neo cassette. An HSV thymidine kinase cassette from pNT (Tybulewicz et al., 1991) was placed at the 5' end of the targeting vector.

PC3 stem cells (O'Gorman et al., 1997) containing a protamine-Cre transgene were transfected with 20 µg of linearized targeting vector and subjected to selection with G418 and ganciclovir according to standard protocols (Hasty et al., 1991). Of 60 clones for which informative Southern blots were obtained, 8 were found to be homologously recombined at the *Pbx3* locus. Subsequent PCR analyses determined that 3 of these contained the 5' loxP site. Additional Southern and PCR analyses confirmed that the recombinant alleles had the predicted structure. Two clones were injected into C57BL/6 blastocysts and the resulting chimeras were crossed to C57BL/6 females. The protamine-Cre transgene present in PC3 ES cells causes Cre-mediated recombination of target sequences in approximately 90% of male germ cells (O'Gorman et al., 1997). PCR analyses showed that the majority of the homologously recombined

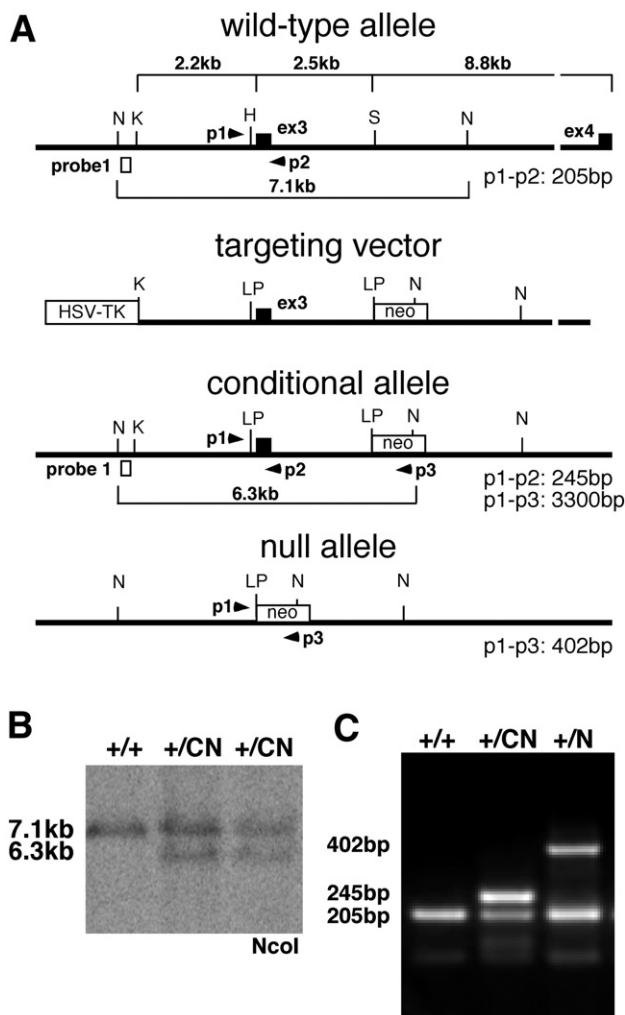


Fig. 1. Generation of *Pbx3C* and *Pbx3N* alleles. (A) Schematic representation of the *Pbx3* genomic locus, the targeting vector, and the *Pbx3C* conditional and *Pbx3N* null alleles. The black box indicates exon (ex) 3 and 4. The positions of the loxP sites (LP), the neomycin (neo) and thymidine kinase (HSV-TK) cassettes, and the hybridization probe (probe1) and PCR primers (p1–3) used for genotyping analyses are shown. Brackets indicate the sizes of *NcoI* restriction digest fragments and PCR amplification products. (B) Southern blot of *NcoI*-digested genomic DNA from control (+/+) ES cells and two independently targeted +/*Pbx3C* (+/CN) ES clones showing wild-type (+/+, 7.1 kb) and homologously recombined (+/*Pbx3C*, 6.3 kb) products labeled by probe 1 (A). (C) PCR analysis of tail DNA from wild type (+/+), +/*Pbx3C* (+/CN) and +/*Pbx3N* (+/N) mice. The product generated by primers p1 and p2 from the *Pbx3C* allele is 40 bp larger than that from the wild-type allele because of the loxP site. Primers 1 and 3 are 3.3 kb apart in the conditional allele and generate a product of 402 bp from the Cre-recombined null allele.

*Pbx3* alleles recovered from progeny of chimeras had lost exon3 and were presumptive null alleles (*Pbx3N*). A minority of the alleles we not recombined by Cre and were presumptive conditional alleles (*Pbx3C*). Mice homozygous for the *Pbx3N* allele died at birth and the allele was maintained through intercross matings. Mice homozygous for the *Pbx3C* allele were grossly indistinguishable from +/*Pbx3C* and +/+ littermates and the allele was maintained as a homozygous stock. Additional crosses generated males heterozygous for the *Pbx3C* allele and homozygous for a recombinant allele of *Hoxb1*, referred to as the *B1Cre* allele, in which the normal coding sequence had been replaced by that for Cre recombinase (O’Gorman, 2005). Most of the mice studied here were the progeny of +/*Pbx3C*:*B1Cre*/*B1Cre* males and *Pbx3C*/*Pbx3C*:+/+ females. Mice heterozygous for the *B1Cre* allele and homozygous for the *Pbx3C* allele (*Pbx3C*/*Pbx3C*:+/*B1Cre*) are here referred to as *Pbx3C*/*B1* mutants.

### Behavioral testing

Accelerating rotarod testing was used to assess the gross motor abilities of 1- and 2-month-old *Pbx3C*/*B1* mutant mice ( $N=17$ ) and littermate controls (+/*Pbx3C*:+/*B1Cre*,  $N=18$ ). At 1 month, mice were trained for three consecutive days and then tested on the fourth and fifth days. On day 1, mice were given trials at 2 rpm ( $2 \times 2$  min) and 4 rpm ( $1 \times 2$  min). On day 2, mice were given trials at 2 rpm ( $1 \times 2$  min) and 4 rpm ( $2 \times 2$  min). On day 3, mice were given trials at 2 and 4 rpm ( $1 \times 2$  min each) and three accelerating trials in which the speed of the rotarod started at 1 rpm and increased by 0.75 rpm every 30 s. The latency to fall was measured in 6 accelerating trials on days 4 and 5 (3 each day). At 2 months of age the same animals were re-trained with the day 3 training protocol and a second data set was collected from six accelerating trials performed over 2 days. All data were analyzed using a one-tailed *t*-test.

Several behavioral tests were used to assess sensation of *Pbx3C*/*B1* mutant and littermate control mice at 2 months of age. Sensitivity to mechanical stimulation was assessed by determining 50% response thresholds to a set of von Frey filaments (0.16–2.0 g stiffness) using the Dixon up–down method (Chaplan et al., 1994). Mice were placed in wire mesh cages and allowed to acclimatize for approximately 15 min. Filaments were applied to the plantar surface of the hindpaw with enough force to bend the filament and held for 3 s, starting with three trials with a 0.6 g fiber. These were followed by trials with stiffer fibers when there was no response or less stiff fibers when there was a positive response (brisk paw withdrawal). A hot plate test was used to measure thermal sensitivity. Mice were placed on a 55 °C hot plate for a maximum of 30 s and the time to a response, either jumping or the brisk withdrawal, shaking or licking of a paw, was recorded. Sensitivity to light touch was assessed by the sticky tape assay (Bradbury et al., 2002; Thallmair et al., 1998). Animals were placed in a wire enclosure and acclimatized for 10 min. A one-quarter inch diameter circular sticker was then placed on the plantar surface of the forepaw and the time to commencement of grooming behavior was recorded. All behavioral data were analyzed with a Student’s *t*-test.

### Antibodies and immunohistochemistry

A rabbit polyclonal antibody to *Pbx3* was generated using an amino terminal peptide (MLQTLGAVNLAGHSVQGGM, GenBank NM 016768) that shows substantial sequence divergence from other *Pbx* family members. The antibody was found to be specific for *Pbx3* by two criteria: (1) it did not label cells in *Pbx3* null mice (not shown) and labeled very few cells in *Pbx3C*/*B1* mutant mice (Fig. 2D), and (2) double labeling with the antibody and an *in situ* probe for *Pbx3* mRNA in chick spinal cord showed complete overlap of the two signals (not shown). For antibodies to Meis1, the coding sequence (GenBank NM 010789) was amplified from a mouse cDNA library and a fragment encoding the first 228 amino acids was subcloned in pGEX4 and the derived GST fusion protein was used to generate antibodies in guinea pigs.

Postnatal mice were anesthetized with Avertin and perfused transcardially with PBS followed by 4% paraformaldehyde in sodium phosphate buffer. Embryos were fixed by immersion for 1–3 h in the same fixative. Dissected tissues were washed in PBS overnight at 4 °C, equilibrated with 30% sucrose in PBS, and frozen in OCT (Tissue-Tek) for sectioning. Sections were blocked with 10% normal donkey serum in PBST (PBS plus 0.2% Triton) and primary antibodies were applied overnight at 4 °C. Primary antibodies included rabbit  $\alpha$ -calbindin (1:250; Chemicon), goat  $\alpha$ -ChAT (1:500; Chemicon), guinea pig  $\alpha$ -parvalbumin (1:500; Chemicon), mouse  $\alpha$ -NeuN (1:2500; Chemicon), rabbit  $\alpha$ -PKC- $\gamma$  (1:1000; Santa Cruz), rabbit  $\alpha$ -calretinin (1:1000; Sigma), mouse (1:100; Developmental Studies Hybridoma Bank (DSHB)) and guinea pig  $\alpha$ -Islet1/2 (1:6000; generous gift of Samuel Pfaff), rabbit  $\alpha$ -Pax2 (1:500; Abcam), rabbit and guinea pig  $\alpha$ -Tlx3 (1:10,000; generous gift of Thomas Muller), rabbit and guinea pig  $\alpha$ -Lmx1b (1:10,000; T. Muller), guinea pig  $\alpha$ -Chx10 (1:10,000; S. Pfaff), mouse  $\alpha$ -Nkx2.2 and  $\alpha$ -Evx1 (1:100; DSHB), rabbit  $\alpha$ -*Pbx3* (1:800) and  $\alpha$ -panMeis1 (1:1000). Secondary antibodies (Jackson Immunochemicals) were applied for 2 h.

### Quantification

Histological material was examined and photographed with either a Zeiss Axioskop equipped with a Hamamatsu digital camera and Openlab software

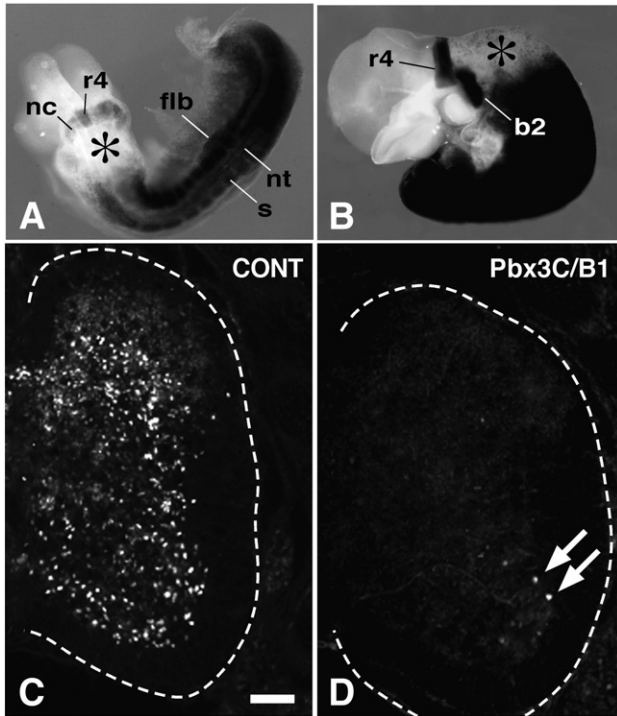


Fig. 2. Cre expression from the *B1Cre* allele. (A, B)  $\beta$ -galactosidase histochemistry of E9.25 (A) and E10.5 (B) *+B1Cre; +R26R* embryos. At approximately E9.25 (A), activation of the *R26R* allele was observed in most tissues caudal to the hindbrain, including the neural tube (nt), somites (s), lateral plate mesoderm, and the forelimb bud (flb). Activation was also seen in r4 and the neural crest emerging from r4 (nc). By E10.5 (B) strong activation was seen in rhombomere 4 and the second branchial arch (b2). Only low levels of recombination were seen in the caudal hindbrain at either stage (\*). (C, D) Cross sections of brachial spinal cord (outlined) from E15.5+*B1Cre* embryos that were either *+Pbx3C* (C) or *Pbx3C/Pbx3C* (D) labeled with an antibody to Pbx3. Pbx3 expression is virtually eliminated in the *Pbx3C/B1* mutant embryo except for a small numbers of motor neurons that continued to express (arrows, D). Scale bar: (C, D) 100  $\mu$ m.

(Improvisation), or with a Zeiss LSM 510 confocal microscope. The quantification of areas in the adult spinal cord was performed using five sections spaced at 50  $\mu$ m intervals from the C8 vertebral level, as determined by the position of the dorsal nerve root, from each of three control and three mutant animals. Quantification of dorsal horn neuron numbers was done by determining the number of DAPI-positive nuclei within calbindin-, calretinin-, parvalbumin- or NeuN-positive cellular profiles of adult mutant and control mice using five sections from each of three animals. For quantification of calbindin(+) neurons in E15.5 brachial spinal cord, the sections used were those immediately rostral to the first rib. Calbindin(+) neuronal cell bodies were counted on at least five sections in three control and mutant embryos. For the position of Meis(+) and Pax2(+) cell bodies as a function of distance from the pial surface, Openlab software was used to impose a  $100 \times 300 \mu$ m grid on images of five sections for each of three wild-type and mutant embryos and the numbers of DAPI(+) and either Meis(+) or Pax2(+) profiles in each of 5 adjacent 60  $\mu$ m bins were determined.

#### *In situ* hybridization

Probes for Slc17a6 (vesicular glutamate transporter 2 (VGLUT2), bp 2002–2728, GenBank NM080853), and Slc32a1 (vesicular inhibitory amino acid transporter (VIAAT), bp 1926–2583, GenBank NM009508) were amplified from mouse genomic DNA. PCR products were cloned into TOPO-pCR4. Digoxigenin-labeled riboprobes were synthesized using a labeling kit according to the manufacturer's instructions (Roche). Embryos were harvested and fixed as

described above for immunohistochemistry under RNase-free conditions. *In situ* hybridization was performed as previously described (Schaeren-Wiemers and Gerfin-Moser, 1993).

## Results

### *Elimination of Pbx3 function by a Hoxb1-Cre allele*

Transmission of the *Pbx3C* allele through the germline of chimeras prepared with targeted PC3 embryonic stem cell clones (O'Gorman et al., 1997) resulted in the recovery of both a Cre-recombined null allele (*Pbx3N*) and the original conditional allele (*Pbx3C*) (Fig. 1). Both the null and conditional alleles were transmitted in normal Mendelian ratios but, as previously described for another *Pbx3* null mutation (Rhee et al., 2004), animals homozygous for the *Pbx3N* allele became cyanotic immediately after birth and died. In contrast, mice homozygous for the conditional allele were grossly indistinguishable from littermate controls, reproduced well, and have been maintained as a homozygous line.

To eliminate *Pbx3* function in tissues below cervical levels while sparing expression in the caudal hindbrain, we used a Cre-expressing allele of *Hoxb1*, which we refer to as *B1Cre*. In this allele the first exon of *Hoxb1* was replaced by the *Cre* coding sequence, which was expected to create a null allele of *Hoxb1* that expressed Cre instead. The wild-type *Hoxb1* allele is transiently expressed in virtually all ectodermal, endodermal, and mesodermal tissues below cervical levels between E8.75 and E10.75, after which expression ceases (Frohman et al., 1990; Murphy et al., 1989). It is also expressed at very high levels in rhombomere 4 (r4) of the hindbrain during this period, but at very low levels in the caudal hindbrain.

To determine the spatial and temporal pattern of Cre expression from the *B1Cre* allele, we generated mice heterozygous for *B1Cre* and for the Cre-conditional *R26R* reporter allele that expresses  $\beta$ -galactosidase after Cre-mediated recombination (Soriano, 1999). In these *+B1Cre; +R26R* embryos,  $\beta$ -galactosidase expression was clearly evident at E9.0–E9.5 in somitic, presomitic, and lateral plate mesoderm posterior to the hindbrain, and in r4 of the hindbrain and the neural crest emerging from r4 to migrate into the second branchial arch (Fig. 2A). At this early time point, approximately 6–12 h after the onset of *Hoxb1* expression from the endogenous allele, a substantial fraction of the cells in each of these tissues expressed moderate levels of the marker. The number of cells expressing the marker and the level of marker expression from the Cre-recombined allele increased dramatically over the ensuing 24 h, so that by E10.5 virtually all cells in these tissues and their derivatives expressed high levels of the marker (Fig. 2B). In sectioned material from E10.5 embryos labeled with antibodies to  $\beta$ -galactosidase, high levels of marker expression were observed in virtually all cells in tissues below the level of the hindbrain, including the spinal cord, the peripheral nervous system, the axial and appendicular musculature, and mesenchymal tissues (Fig. 2B and data not shown). As Cre-mediated recombination is irreversible under these conditions, the marker allele remained in the activated state throughout all subsequent stages of

embryonic and adult life, although levels of  $\beta$ -galactosidase expression varied widely as tissues matured. In an extensive series of embryos ranging from E9.5 to E18.5 that contained both the B1Cre and R26R alleles, we have not observed evidence of additional Cre-mediated recombination in the caudal hindbrain, neural tissues anterior to r4, or in craniofacial tissues anterior to the second branchial arch.

Given these data, we anticipated that combining the conditional Pbx3C allele with the B1Cre allele would lead to the irreversible inactivation of the conditional allele in most tissues posterior to cervical levels by E10.5, resulting in the loss of Pbx3 function in these tissues. In wild-type embryos, Pbx3 is robustly expressed by multiple tissues at midgestational stages, including neural tissues, the limbs, and rib primordia (Di Giacomo et al., 2006). In Pbx3C/B1 mutant embryos, homozygous for the Pbx3c allele and heterozygous for the B1Cre allele, we found that Pbx3 expression virtually eliminated throughout the domain of R26R marker expression observed in +/B1Cre;+/R26R embryos at E10.5 (Fig. 2B). Importantly for the behavioral phenotype described below, this included both central and peripheral neural tissues, the periaxial musculature, and the limb buds.

In the spinal cord of wild-type embryos, Pbx3 was expressed in a variety of postmitotic cells at multiple dorsoventral levels, but was not expressed by proliferating cells within the ventricular zone. Expression was first evident at E10.75 in ventral motor neurons and a small number dorsal neurons (Supplementary Fig. 1, and data not shown). At E15, Pbx3 expression was observed in postmitotic neurons at all levels of the spinal cord (Fig. 2C), but the number of expressing cells did not increase markedly after E15.5. In Pbx3c/B1 mutant embryos, by contrast, Pbx3 expression was eliminated from all neurons of the spinal cord except for a few neurons in the ventral horn (Fig. 2D). Additional material showed that the loss of Pbx3 expression was obvious as early as E10.75 (Supplementary Figs. 1C, G–I, and data not shown).

#### *Behavioral phenotype of Pbx3C/B1 mutant mice*

Pbx3C/B1 mutants developed a profound movement disorder that became apparent during the fourth postnatal week. At 2 weeks of age the mutants, previously indistinguishable from their littermates by external observation, could be identified by their small size. By 4 weeks of age, the mutants consistently displayed hypokinesia, splaying of the hind limbs, and extensor posturing of the limbs and tail at rest (Figs. 3A, B; Supplementary movie). Initially, the extensor posturing was most consistently seen in the forelimbs, which the mutants often elevated above the supporting surface for prolonged periods when not moving (>20 s). By 10 weeks of age the mutants also consistently elevated their hind limbs. They walked with a normally alternating gait, but their hind limb placement was wider than that of controls. When picked up by their tails the mutants would briefly splay their limbs as the controls did, but then rapidly clasped both forelimbs and hind limbs. Pbx3C/B1 mice showed a strong startle response to noise, and an immediate and vigorous righting reflex when placed on their backs. As they

aged their hind limb placement became broader and by 4 months they often dragged their abdomens on the supporting surface. There was little further progression of the movement disorder in the small number of mutants that we maintained for up to 8 months, but their overall health declined, probably reflecting difficulties they had with feeding and grooming.

To quantify the deficits in locomotion, mice were tested on an accelerating rotarod at 4 and 8 weeks of age. Rotarod performance of Pbx3C/B1 mice was significantly impaired when compared to littermate controls at both time points ( $p < 0.001$ ) (Fig. 3C). Additionally, the mutants demonstrated a significant decline in performance between 4 and 8 weeks ( $p < 0.001$ ), establishing that the movement disorder was progressive. Mechanical and thermal sensation was tested to determine if the mutants elevated their limbs because of allodynia. We instead found that 8-week-old Pbx3/B1 mutants showed reduced sensitivity to noxious stimuli. The sticky tape assay demonstrated that touch sensation in Pbx3C/B1 mutants was significantly impaired ( $p < 0.01$ ); on average they took three times as long as controls to sense the presence of the tape and begin grooming (Fig. 3D). The mutants were also severely impaired in thermal sensation as assessed by the hot plate test ( $p < 0.001$ ) (Fig. 3E). Only one of eight mutants responded with a brisk paw withdrawal or licking within 30 s of being placed on the hot plate, in contrast to all seven of the controls. Finally, the mutants demonstrated a tendency towards impaired mechanical sensation in the von Frey fiber test, although this did not reach statistical significance ( $p = 0.13$ ) (Fig. 3F). The reduced sensitivity to noxious stimuli observed in Pbx3C/B1 mutants makes it unlikely their altered postures were caused by allodynia.

It is unlikely that the phenotypes described below were attributable to alterations of *Hoxb1* function. Although the B1Cre allele is null for *Hoxb1* function, mice heterozygous for other null alleles of *Hoxb1* are phenotypically normal, and homozygous mutants do not have abnormal postures or locomotion (Goddard et al., 1996; Studer et al., 1996). This was confirmed by rotarod testing in which mice homozygous for the B1Cre allele used here did not show any deficits (data not shown).

#### *Spinal cord morphology of adult Pbx3C/B1 mutant mice*

The B1Cre allele does not lead to Cre expression in higher motor centers in the cerebrum, midbrain or cerebellum, and we and others have not observed changes in the musculoskeletal or peripheral nervous systems of late-stage embryos homozygous for constitutively null alleles *Pbx3* (Rhee et al., 2004). The peripheral innervation of the limbs of E18.5 *Pbx3*<sup>-/-</sup> embryos was examined by immunohistochemistry with antibodies to the 150-kDa neurofilament isoform of neurofilament on whole mount embryos and sections taken through the distal hindlimb. We found no obvious differences in the overall pattern of innervation in null embryos as compared with controls (Supplementary Fig. 2). Motor end plates labeled with vesicular acetylcholine transporter (VAChT) were also present in approximately normal numbers in null embryos (data not shown). Additionally, although Pbx3C/B1 mutants were smaller than

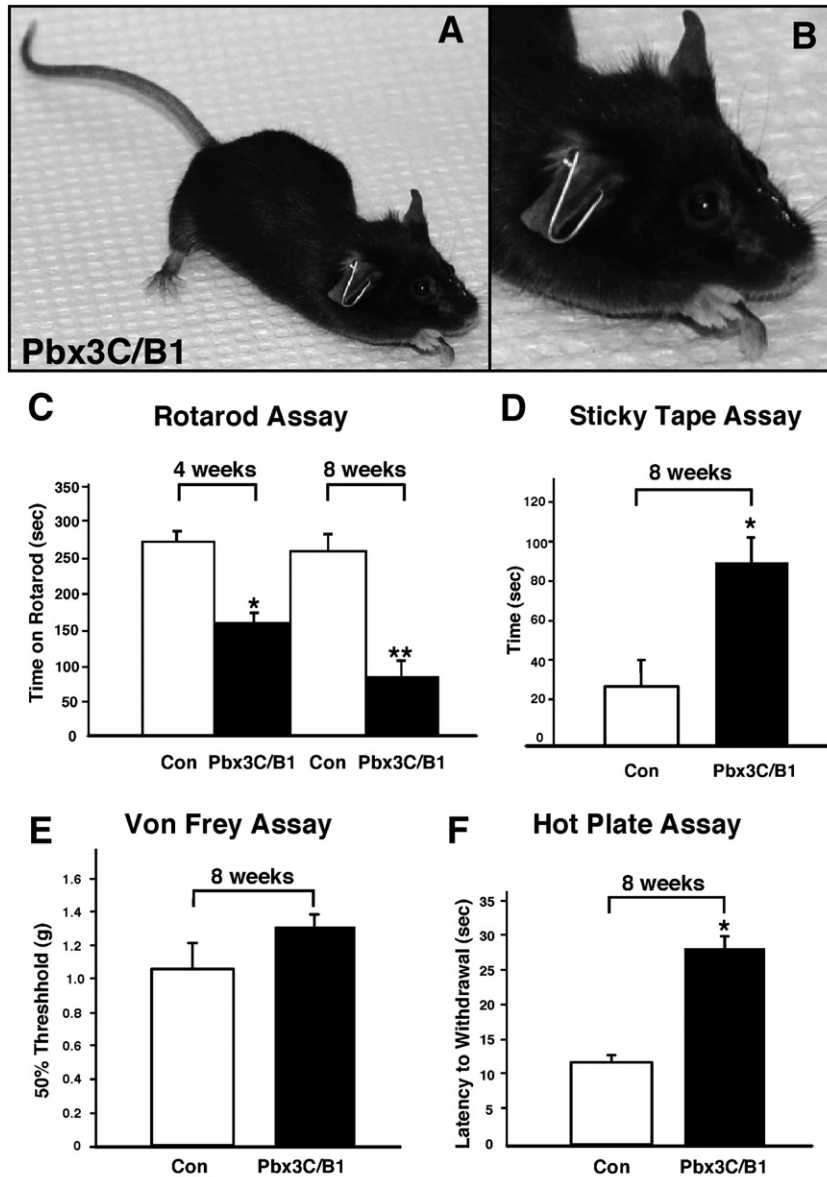


Fig. 3. Abnormal resting postures in adult Pbx3C/B1 mutants. (A, B) A 10-week-old Pbx3C/B1 mutant showing elevation of the forelimbs above the supporting surface at rest and the characteristically splayed hindlimbs and raised tail. (C) Rotarod testing of 4- and 8-week-old Pbx3C/B1 mutants (black bars) and littermate controls (white bars). The average times of 6 trials is shown and error bars represent S.E.M. (\*)  $p < 0.001$  compared to 4-week control; (\*\*)  $p < 0.001$  compared to 8-week control and 4-week Pbx3C/B1 mutant values (unpaired  $t$ -test (control,  $n = 17$ ; Pbx3C/B1,  $n = 16$ )). (D) Sticky tape testing of 8-week-old Pbx3C/B1 mutants ( $n = 8$ ; black bars) and littermate controls ( $n = 7$ ; white bars). Error bars represent S.E.M. (\*)  $p < 0.01$ . (E) Hot plate test of 8-week-old Pbx3C/B1 mutants ( $n = 8$ ; black bars) and littermate controls ( $n = 7$ ; white bars) for thermosensation. Error bars represent S.E.M. (\*)  $p < 0.001$ . (F) Von Frey assay of 8-week-old Pbx3C/B1 mutants ( $n = 8$ ; black bars) and littermate controls ( $n = 7$ ; white bars) for mechanosensation. Error bars represent S.E.M.

their littermate controls, we found no selective atrophy of the extensor or flexor limb muscles at 8 weeks of age.

We next sought to determine if there were alterations of the spinal cord that could result in the behavioral phenotype. Dark-field microscopy of transverse sections from 10-week-old Pbx3C/B1 spinal cords demonstrated that overall organization and myelination of the cord appeared normal (Figs. 4A, B). At the level of the eighth cervical vertebra (C8) the cross-sectional areas of both grey and white matter were slightly smaller in mutants than in controls (data not shown). The most striking difference was in the cross-sectional area of the dorsal horn, which was markedly smaller in the mutants throughout the

length of the spinal cord ( $p < 0.02$ , Fig. 4C). The atrophy in the dorsal horn made the dorsal funiculus appear flattened and led to slight changes in the shape of the dorsal portion of the lateral funiculus. In contrast, the area of the ventral spinal cord was unchanged in Pbx3C/B1 mutants as compared to controls (Fig. 4D) as were the number of choline acetyl transferase(+) motor neurons and calbindin(+) Renshaw interneurons at the same level (C8) (Supplementary Fig. 3, data not shown).

The atrophic changes in the dorsal horn of mutant embryos appeared to be particularly severe in superficial laminae, which were markedly thinned. Despite the atrophic changes in the mutants, at 10 weeks of age the dorsal horn of both mutants and

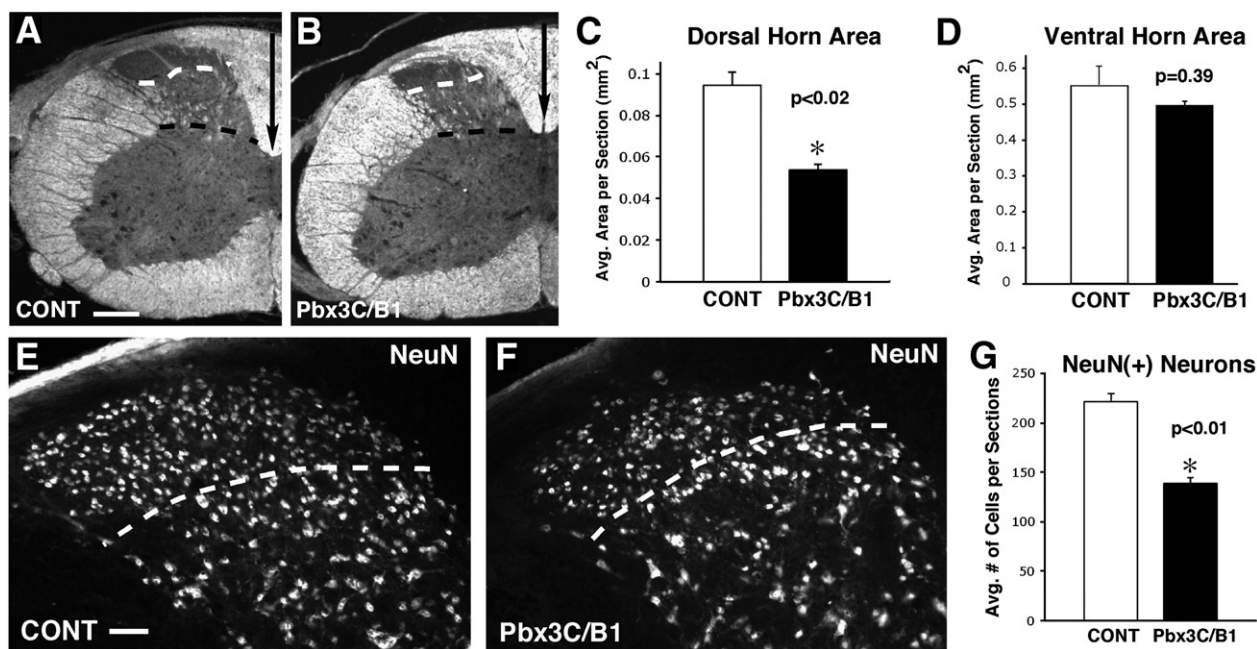


Fig. 4. Neuron loss in the dorsal horn of *Pbx3C/B1* mutants. (A, B) Darkfield photomicrographs of adult C8 spinal cord from control (A) and *Pbx3C/B1* mutant (B) mice. In the mutants, the area of the dorsal horn (above the black dashed line) was decreased, and the reduction appeared particularly severe in the myelin-poor superficial laminae (above the white dashed line). The dorsal funiculus also appeared flattened (arrows). (C, D) Quantification of dorsal horn (C) and ventral cord (D) areas in *Pbx3C/B1* mutant and littermate control mice ( $n=3$  for each, unpaired  $t$ -test). (E, F) NeuN immunohistochemistry showing reduced neuron density and thinning of the superficial laminae (above the white dashed lines) at C8 in *Pbx3C/B1* mutant mice. Neuronal size (E, F) and myelin content (e.g., A, B) were used to distinguish the superficial (approximately laminae I–III) from the deeper (approximately laminae IV–IV) laminae. (G) Histogram of the average numbers of neurons per section in laminae I–III of wild-type and *Pbx3C/B1* mice ( $n=3$  for each, unpaired  $t$ -test). Error bars represent S.E.M. Scale bars: (A, B) 200  $\mu$ M; (C, D) 50  $\mu$ M.

controls could be reliably divided into a superficial portion, that contained high densities of small neurons by NeuN labeling and relatively few myelinated fibers by darkfield microscopy, and a deeper portion that contained a mixture of small and large neurons and many more myelinated fibers (Figs. 4A, B, E, F). To determine the extent of cell loss in the superficial dorsal horn of the mutants we drew a line just above the larger cells of the deeper layers and counted all the NeuN-labeled neurons superficial to it (Figs. 4E, F). This line corresponded to the transition between dorsal laminae III and IV as it was found just ventral to the PKC- $\gamma$ (+) neurons in laminae III on adjacent sections (Ren and Ruda, 1994). We found that there was a significant reduction, of approximately 30%, in the neuron number of the superficial dorsal horn of mutant mice ( $p<0.01$ ) (Fig. 4G).

To determine whether the cell loss in the dorsal horn of *Pbx3C/B1* mice was distributed among multiple classes of neurons or was limited to specific classes, we used several markers that label different classes of dorsal horn neurons (Ren and Ruda, 1994). These classes included calbindin-D28K (laminae I and II), calretinin (inner lamina I and lamina II), parvalbumin (lamina III) and PKC- $\gamma$  (laminae II and III) expressing neurons. In contrast to wild-type mice, in which cell bodies positive for each of these markers formed continuous bands along the whole medio-lateral extent of the dorsal horn, in the mutants the bands were frequently discontinuous (Figs. 5A, B, D, E, G, H). The numbers of cells that expressed calbindin, calretinin, and PKC- $\gamma$  were each reduced in the dorsal horn of *Pbx3C/B1* mutants as compared to littermate controls (Figs. 5C, F, I). The number of parvalbumin(+) cell bodies was too small to gather meaningful

quantitative data. Thus, neuron loss in the dorsal horn of mutants was not restricted to a single class of neurons.

#### *Expression of Pbx3 and Meis proteins in the embryonic mouse spinal cord*

Although *Pbx3* is known to be expressed in the developing spinal cord (Di Giacomo et al., 2006; Rhee et al., 2004), information about the identities of expressing cells has not been reported. Between E10.75, when *Pbx3* expression was first evident by immunohistochemistry, and E15.5, when most neurons of the spinal cord have become postmitotic and have migrated to their eventual positions, we found that *Pbx3* was expressed throughout the rostrocaudal axis in multiple classes of cells and at multiple dorsoventral positions. At these ages, virtually all immunoreactivity was restricted to the nuclei of postmitotic cells; we did not observe more than faint cytoplasmic labeling or any labeling of the mitotically active cells of the ventricular zone. At E10.75 the most prominent expression was in the ventral spinal cord. Double labeling with antibodies to the motor neuron marker *Islet 1/2* demonstrated that *Pbx3* was expressed in some motor neurons at all rostrocaudal levels, and in a small number of additional ventral cells (Supplementary Figs. 1A, B). Labeling with antibodies to *Evx1*, *Chx10*, and *Nkx2.2*, which respectively label V0, V2, and V3 interneurons (Lee and Pfaff, 2001), showed that none of these markers were expressed in *Pbx3*(+) cells (Supplementary Figs. 1D–F). The expression of *Pbx3* in some motor neurons persisted through early postnatal ages (not shown).

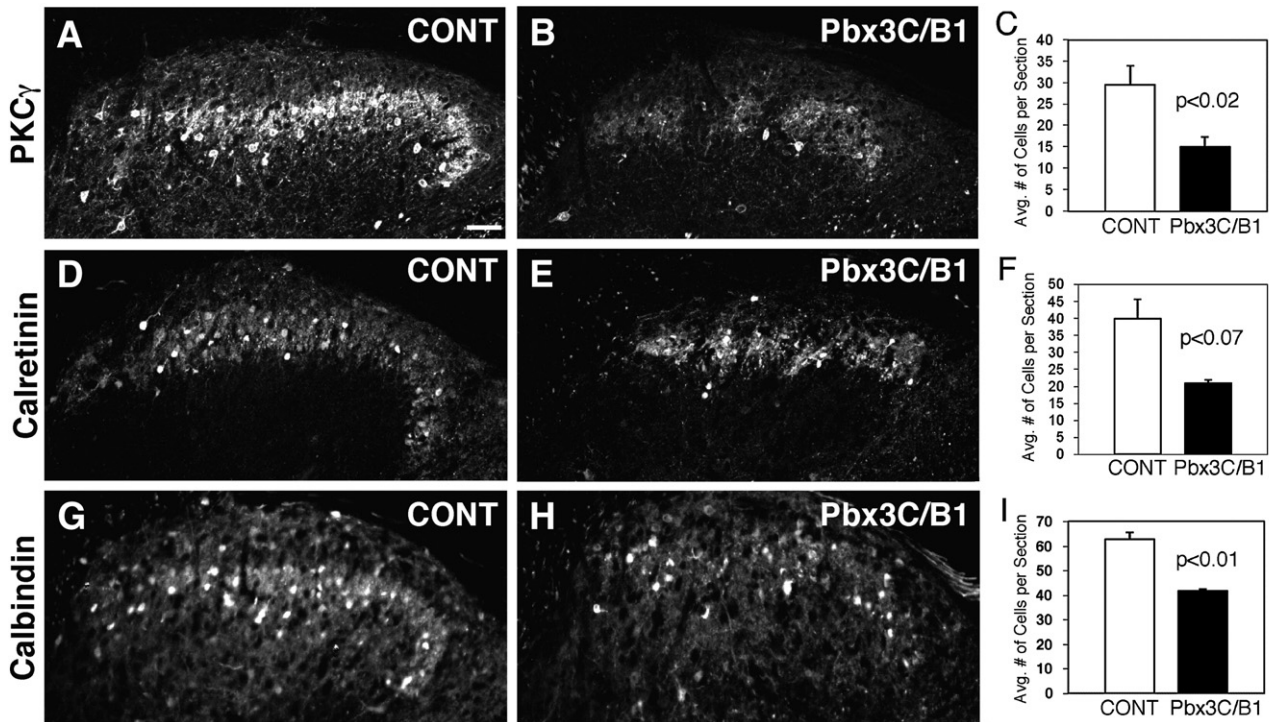


Fig. 5. Alterations in multiple neuron classes in C8 adult dorsal horn of Pbx3C/B1 mutants. Immunohistochemistry of sections from wild-type (A, D, G) and Pbx3C/B1 mutant (B, E, H) mice using antibodies to protein kinase C- $\gamma$  (PKC- $\gamma$ ) (A, B), calretinin (D, E) and calbindin (G, H). The mediolateral continuity of labeled cells was disrupted for each marker in the mutants. (C, F, I) Quantification of the number of PKC- $\gamma$  (C,  $n=3$ ), calretinin (F,  $n=2$ ), and calbindin (I,  $n=3$ ) expressing neurons in the dorsal horn of wild-type and Pbx3C/B1 embryos. The average number of cells per section was determined and significance was calculated using an unpaired *t*-test. Error bars represent S.E.M. Scale bar: 50  $\mu$ M.

In the dorsal cord at E10.75, a few neurons in the lateral cord just above the sulcus limitans expressed Pbx3. Some of these could be identified as early-born, dI3-derived interneurons because they were also labeled with Islet1/2 antibodies (Qian et al., 2001). By E12.5, expression of Pbx3 was observed in many more dorsal neurons (Fig. 6A). These included some early-born Tlx3(+) and Lmx1b(+) neurons that arise from dI5 and migrate laterally (arrows in Figs. 6B, C), and some early-born Lmx1b(-) neurons that arise from dI3 and migrate ventrally (Fig. 6C) (Gross et al., 2002; Muller et al., 2002). At E15.5 Pbx3 was strongly expressed in cells generated in the later phase of neurogenesis that settle in presumptive laminae IV–VI (Fig. 6E). Most of these Pbx3(+) cells coexpressed Lmx1b (Fig. 6G), and a smaller number of the more dorsal Pbx3(+) cells coexpressed Tlx3 (Fig. 6F). Conversely, Pbx3 expression was only seen in some of the cells expressing either of these markers. Others have established that Tlx3 and Lmx1b are coexpressed at E13.5 in most glutamatergic neurons derived from dIL<sub>B</sub>, and that Tlx3 expression is greatly reduced in these same cells, particularly the deeper cells, at slightly later stages (Cheng et al., 2004). Since all dorsal neurons that express Lmx1b or Tlx3 are glutamatergic (Cheng et al., 2004), this coexpression suggested that Pbx3 was expressed in subsets of glutamatergic neurons. The glutamatergic phenotype of Pbx3(+) neurons was confirmed by *in situ* hybridization for the vesicular glutamate receptor VGLUT2 followed by immunohistochemistry for Pbx3 (Fig. 6I). Collectively, these data established that Pbx3 expression was restricted to glutamatergic cells in the dorsal horn of the spinal cord.

Meis proteins were also coexpressed with Pbx3 in neurons of the developing dorsal horn. Meis proteins form multimeric, transcriptionally active DNA-binding complexes with PBC and Hox proteins (Berthelsen et al., 1998; Ferretti et al., 2005; Jacobs et al., 1999), and the heterodimerization of Meis and PBC proteins affects both the stability and the subcellular localization of PBC proteins (Berthelsen et al., 1999; Waskiewicz et al., 2001). Unlike Pbx3, expression of Meis proteins was observed in the majority of cells in the ventricular zone of the dorsal horn (Fig. 6D). Between E10.5 and E15.5, all Pbx3(+) cells throughout the spinal cord coexpressed Meis proteins, but Meis expression was found in many cells that did not express Pbx3 (Figs. 6D, H). To determine the neurotransmitter phenotype of Meis-expressing cells we performed double-label immunohistochemistry with antibodies to Meis and Pax2. Pax2 is expressed by GABAergic cells in the dorsal horn at E13.5 and virtually all cells that do not express Pax2 are glutamatergic (Cheng et al., 2004). We found that the expression of Meis and Pax2 was mutually exclusive (Fig. 6J), and concluded that Meis expression represents a marker for a subset of glutamatergic cells in the dorsal spinal cord at these stages.

#### *Alterations of dorsal horn development in Pbx3/B1 conditionally null mice*

As noted earlier, Pbx3 can first be detected in the spinal cord by immunohistochemistry at E10.75, and even at this stage Pbx3C/B1 mutants had greatly reduced levels of Pbx3 ex-

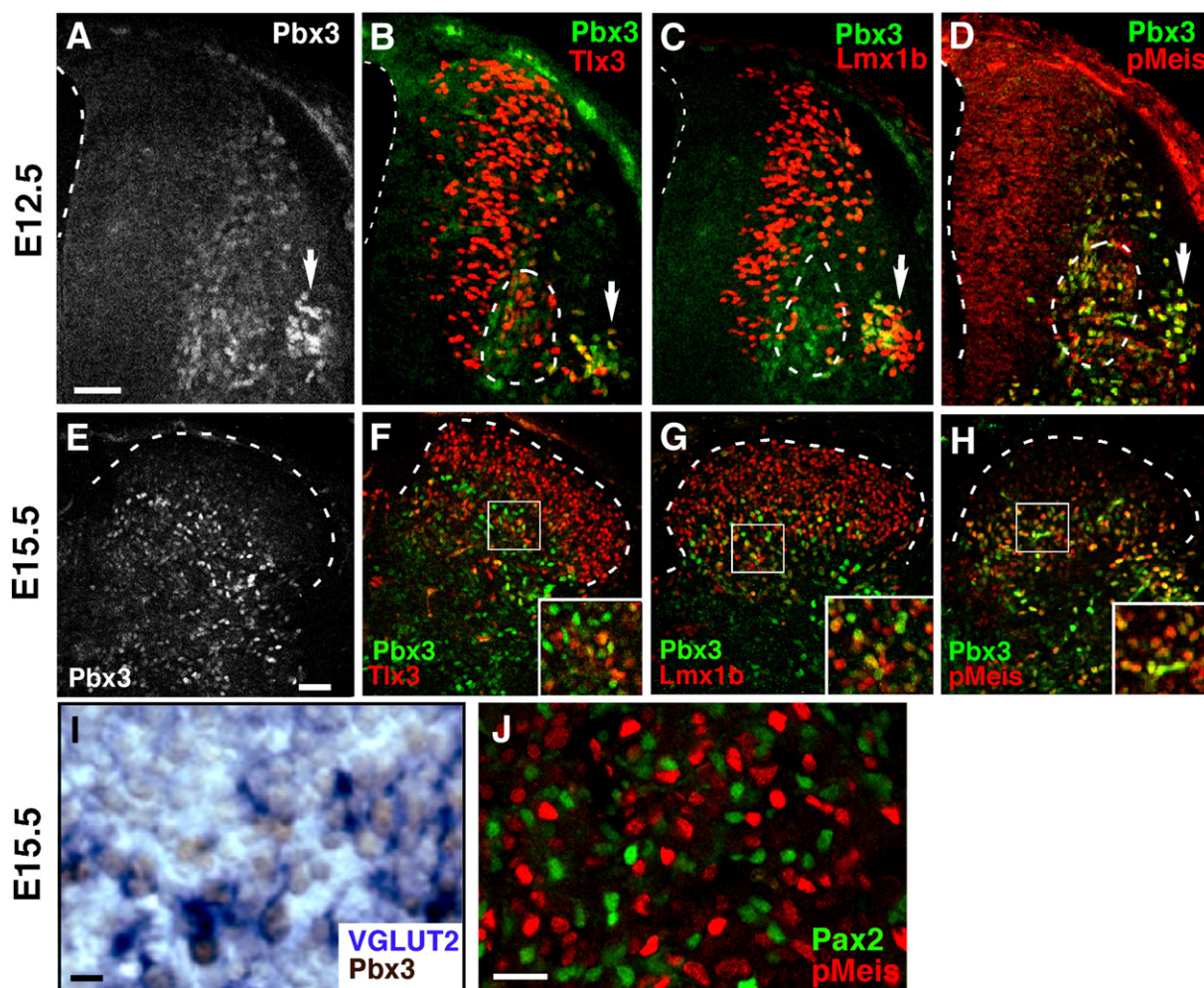


Fig. 6. Pbx3 expression in the dorsal spinal cord at E12.5 and E15.5. (A–H) Immunohistochemistry of control brachial spinal cord with antibodies to Pbx3 and either Tlx3 (B, F) Lmx1b (C, G), or Meis (D, H). At E12.5 Pbx3 was expressed in some of the Tlx3(+), Lmx1b(+) and Meis(+) cells that arise from dI5 and migrate laterally (arrows, A–D) and in some Lmx1b(-), Meis(+) neurons that arise from dI3 and migrate ventrally (dashed circles in panels B–D). Meis was expressed in the ventricular zone and in all Pbx3(+) neurons (D). At E15.5 Pbx3 was strongly expressed in some neurons of the deep dorsal horn and weakly in some superficial neurons (E–H). All Pbx3(+) neurons also expressed Lmx1b (G) and Meis (H). Tlx3 expression was reduced in deeper layers at E15.5 but was still apparent in some Pbx3(+) neurons (F). (I) Immunohistochemistry for Pbx3 (brown) and *in situ* hybridization for VGLUT2 (blue) showed Pbx3(+) cells were glutamatergic. (J) At E15.5 expression of Pax2 (green) and Meis (red) was mutually exclusive. Scale bars: (A–F) 50  $\mu$ M; (G) 10  $\mu$ M; (H) 25  $\mu$ M.

pression (Supplementary Fig. 1). The B1Cre allele eliminated virtually all Pbx3 expression in the spinal cord with the exception of a few motor neurons (Figs. 2C, D). At E10.75 the early specification of motor neurons and V0, V1, V2 and V3 interneurons did not appear to be affected in Pbx3C/B1 mutants (Supplementary Fig. 1, data not shown).

The fact that Pbx3 was expressed in dorsal neurons at stages when the neuronal organization of the dorsal horn is being established raised the question of whether its absence in mutant embryos alters the development of the dorsal horn. Given the common respiratory phenotype of *Tlx3* and *Pbx3* null animals and the restriction of Pbx3 expression to glutamatergic neurons, we examined the distribution of glutamatergic and GABAergic markers in Pbx3C/B1 mutants at E12.5 and E15.5 (Fig. 7). Immunohistochemistry with antibodies to Lmx1b and Tlx3, expressed by glutamatergic cells (Cheng et al., 2004), labeled similar numbers of cell bodies in mutant and control embryos (Figs. 7A, B; data not shown). The amount of *VGLUT2* mRNA

also appeared to be similar in both (Figs. 7E, F). Immunohistochemistry with a Pax2 antibody (Figs. 7C, D) and *in situ* hybridization with probe for *VIAAT* mRNA (data not shown), failed to reveal large differences in the number of inhibitory interneurons (Cheng et al., 2004). These findings establish that Pbx3 is not uniquely required for neurons of the dorsal horn to acquire glutamatergic or GABAergic phenotypes.

Despite the relatively unchanged overall level of *VGLUT2* hybridization signal (Figs. 7E, F), there was a consistent reduction of signal in the deeper dorsal horn (presumptive lamina IV, Figs. 7G, H). Given that Pbx3 was expressed in a small fraction of the entire glutamatergic population but a much larger fraction of Meis(+), glutamatergic neurons, we asked if the distribution of Meis(+) cells was altered in mutant embryos. In E15.5 control embryos, Meis(+) neurons were predominantly located in deeper levels of the dorsal horn. In Pbx3C/B1 mutants there was an increase in the number of Meis(+) neurons at superficial levels (Figs. 8A–D). Quantification showed that

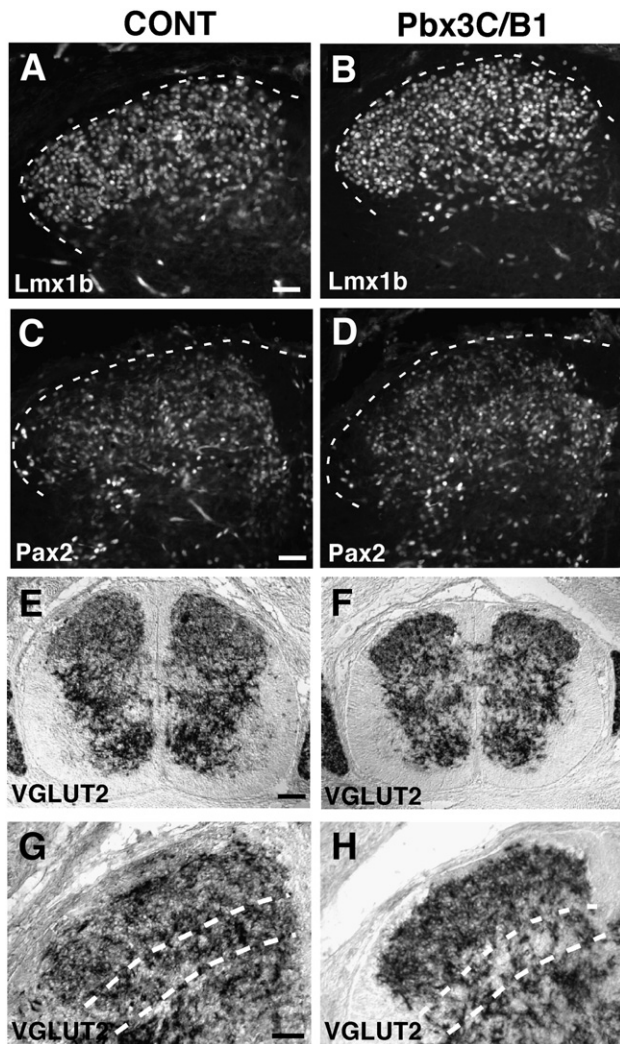


Fig. 7. Dorsal glutamatergic and GABAergic neurons are specified in Pbx3C/B1 animals in approximately normal numbers. (A–D) Immunohistochemistry of E15.5 control (A, C) and Pbx3C/B1 mutant (B, D) brachial spinal cord with antibodies to either Lmx1b to mark glutamatergic neurons (A, B) or Pax2 to mark GABAergic neurons (C, D). The numbers and gross distribution of these markers were similar in mutant and control embryos. (E–H) *In situ* hybridization of E15.5 control (E, G) and Pbx3C/B1 mutant (F, H) brachial spinal cord with probe specific to VGLUT2. While the overall level of VGLUT2 signal in Pbx3C/B1 mutant was similar to controls, it appeared that the level of signal was reduced in the deeper levels of the dorsal horn (dashed lines, G, H). Scale bars: (A–D, G–H) 50  $\mu$ M; (E, F) 100  $\mu$ M.

the increase in superficial neurons was accompanied by a decrease in deeper Meis(+) neurons, without alteration of the total number of Meis(+) neurons (Fig. 8E). We then asked whether this shift was accompanied by any change in cells that expressed GABAergic markers, but found no corresponding difference in the position of Pax2(+) neurons (Supplementary Fig. 4).

Because the numbers of several classes of dorsal horn neurons were reduced in adult Pbx3C/B1 mice, we asked if the appropriate number of neurons were generated initially. At E15.5, when spinal neurogenesis is largely completed and most dorsal horn neurons have completed their initial migrations (Ding et al., 2004; Gross et al., 2002; Muller et al., 2002), there

was no obvious difference in the size of the dorsal horn or the density of DAPI-stained nuclei. Of the markers that showed marked differences in adults, only calbindin was expressed in cell bodies of the dorsal horn at E15.5. Surprisingly, given the reduction observed in adults, the number of calbindin(+) neurons in Pbx3C/B1 mutant embryos was increased by approximately three-fold ( $p < 0.001$ ) and there was a corresponding increase in the amount of calbindin signal within axons in the dorsal portion of the lateral funiculus (Figs. 9A–C). We additionally found that many of these calbindin(+) neurons were also Meis(+) (Fig. 9D). The mispositioning of Meis(+) neurons and the expression of calbindin in an unusually large number of dorsal neurons at E15.5 suggest that the cellular organization of the dorsal horn is altered at relatively early stages of its development, before signs of neuronal loss become evident.

#### *Primary sensory modalities in Pbx3C/B1 conditionally null mice*

A possible explanation for the disorganization of the dorsal horn in Pbx3C/B1 embryos and postnatal mice is that it results from changes in the central projections of dorsal root ganglion (DRG) neurons. To address this possibility, we examined expression profile of Pbx3 in DRG neurons at E15.5, E17.5 and P0. At E15.5 and E17.5, Pbx3 expression in DRG neurons was not clearly above background by immunohistochemistry (Supplementary Fig. 5A, data not shown). At P0, expression was observed in a subset of DRG neuronal nuclei (Supplementary Fig. 5B).

We therefore asked whether the observed changes in dorsal horn morphology were preceded by any gross changes in DRG neurons or their central axons in the mutants. At P0, when cell loss in the mutant brachial dorsal horn had not yet become obvious, the size of the corresponding spinal ganglia and the number of neurons labeled with Islet1/2 antibodies were comparable in mutants and controls (Supplementary Fig. 5). Similar numbers of proprioceptive (parvalbumin(+)) and cutaneous (CGRP(+)) sensory neuronal cell bodies were evident in each (Supplementary Figs. 5C, D). In both mutants and controls, parvalbumin was present in large cell bodies at the ganglionic periphery and CGRP was present in both small and large neurons throughout the ganglia. By P15, we found that the numbers of calbindin(+) and PKC- $\gamma$ (+) neurons in laminae I–III of the C8 dorsal horn were reduced in the mutants (Figs. 10A–D). Despite the clear changes in the dorsal horn, the C8 DRG appeared grossly normal in size and cellular content at this age. The number and distribution of proprioceptive neurons (Figs. 10E, F) and cutaneous sensory neurons (Figs. 10G, H) were comparable in Pbx3C/B1 mutants and controls. Calbindin(+) cell bodies are present in both the dorsal horn and the DRG, yet despite the reductions observed in the dorsal horn, there was no evidence of a significant loss of calbindin(+) DRG neurons (Figs. 10E, F).

Alterations in the distribution of some primary afferent axons became apparent by P15 in the mutants, at approximately the same time as the loss of dorsal horn neurons became apparent. At E15.5, the distribution of DRG afferents within the dorsal

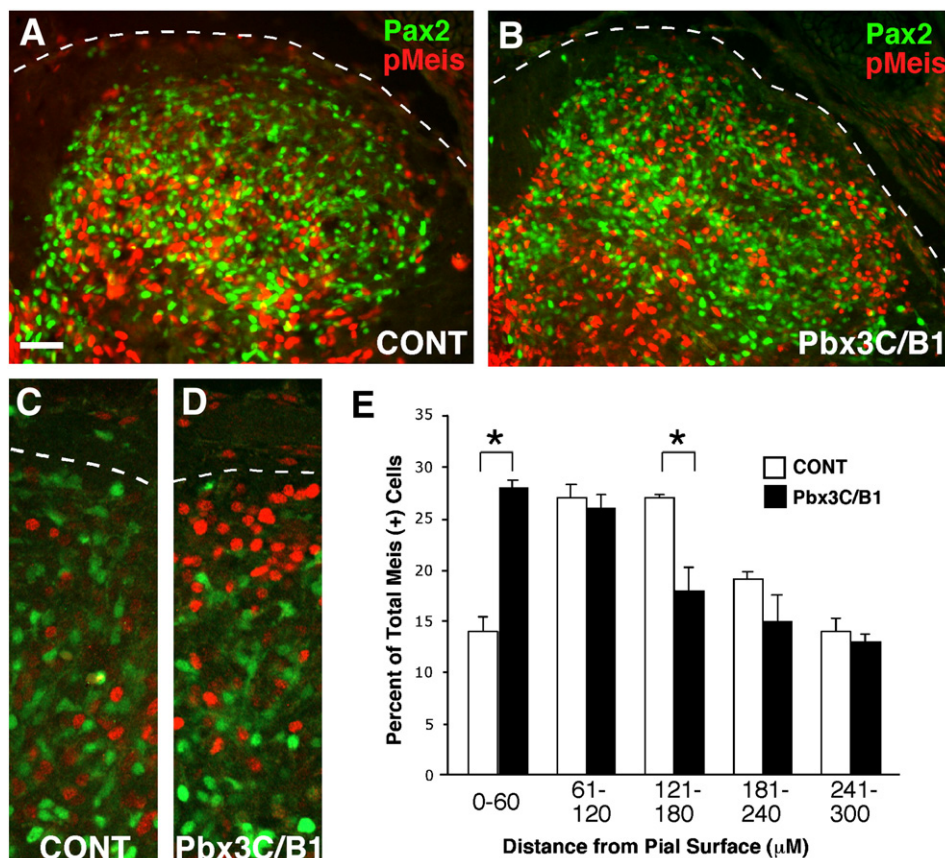


Fig. 8. Meis-expressing glutamatergic neurons assume more superficial positions in *Pbx3C/B1* mutants. (A–D) Immunohistochemistry of E15.5 control (A, C) and *Pbx3C/B1* mutant (B, D) brachial spinal cord with antibodies to Meis (red) and Pax2 (green). While the total number of Meis(+) neurons did not differ between mutants and controls, there was a shift in the position of these cells from deeper to more superficial layers in *Pbx3C/B1* embryos. (E) Quantification of the change in position of Meis(+) cells. The number of Meis(+) cells at different depths is plotted for *Pbx3C/B1* (black bars) and control (white bars) embryos. (\*)  $p < 0.01$ , ( $n = 3$ ) unpaired  $t$ -test. Error bars represent S.E.M. Scale bars: (A, B) 50  $\mu\text{m}$ .

horn of mutant embryos could not be distinguished from that in controls. Proprioceptive, parvalbumin(+) axons entered the dorsal horn at medial positions, while cutaneous, CGRP(+) axons were gathered at the surface of the dorsal horn more laterally (data not shown) (Chen et al., 2006). In both mutant and control embryos, proprioceptive afferents reached positions ventral to the sulcus limitans by E15.5, and by P0 they branched extensively in the ventral spinal cord to form a diffuse plexus around lamina IX motor neurons (Figs. 11A, B). Their appearance remained unchanged at P15. We did note that parvalbumin(+) axons appeared to fasciculate in larger bundles as they passed through the dorsal horn, but this was not correlated with alterations in their eventual terminations within ventral spinal cord.

In contrast to proprioceptive afferents, many of the cutaneous sensory axons did not terminate correctly in the dorsal horn of *Pbx3C/B1* mutants at P15, despite an apparently normal initial distribution. At P0, CGRP(+) fibers formed a diffuse plexus in laminae I–III that was similar in *Pbx3C/B1* mutants and controls (Figs. 11A, B). By P15, many more CGRP(+) fibers extended beyond the superficial laminae of the dorsal horn in the mutants (Figs. 11C, D). These frequently formed thickened fascicles running along the lateral margin of the dorsal funiculus to reach the midline (arrow, Fig. 11D). Additional

thick fascicles of CGRP(+) fibers traversed the superficial laminae at various mediolateral positions and then turned medially to run in a relatively straight trajectory to the midline just ventral to the dorsal funiculus (arrowhead, Fig. 11D). None of the trajectories followed by CGRP(+) fibers in the mutants were truly ectopic, for in control mice one or a few axons were often observed in the same locations (Fig. 11C). The principal difference between the mutants and controls was that the number of fibers passing beyond the superficial laminae was elevated in the mutants. Thus, even though alterations in the neuronal organization of the dorsal horn become evident by midgestation, the distribution of cutaneous sensory afferent axons was not clearly changed until postnatal stages, when the loss of the neuronal targets for these fibers is apparent.

## Discussion

In the present study we have used conditional gene ablation to uncover a novel role for the *Pbx3* Hox gene cofactor in the organization and function of neural circuits essential for normal sensation and locomotion. *Pbx3C/B1* mice, which lack *Pbx3* function in most tissues below cervical levels, had reduced sensitivity to mechanical and thermal stimuli, and showed progressive deficits in posture and locomotion that first became

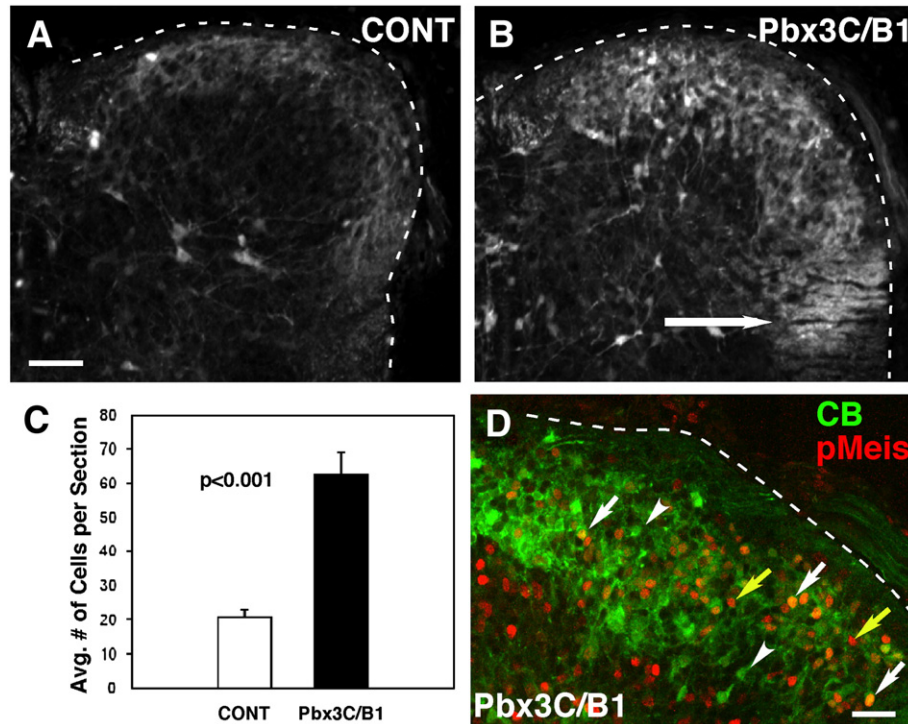


Fig. 9. Increased calbindin expression in Pbx3C/B1 mutant embryos. (A, B) Sections of E15.5 Pbx3C/B1 (B) and littermate control (A) brachial spinal cord labeled with an antibody to calbindin. Total calbindin immunoreactivity was greatly increased in superficial dorsal horn neurons and in axons in the lateral funiculus (arrow). (C) Quantification of the number of calbindin(+) neurons in Pbx3C/B1 (black bars) and littermate controls (white bars) ( $n=3$ , unpaired  $t$ -test). (D) Immunohistochemistry of E15.5 Pbx3C/B1 brachial spinal cord with antibodies to calbindin and Meis. Many superficial Meis neurons expressed calbindin (white arrows), but cells were present that expressed Meis (yellow arrows) or calbindin (arrowheads) alone. Error bars represent S.E.M. Scale bars: (A, B) 50  $\mu$ M; (C) 20  $\mu$ M.

apparent at approximately 4 weeks of age. These behavioral changes were accompanied by marked changes in the morphology of the dorsal horn of the spinal cord that included substantial reductions in the numbers of several neuron classes and alterations in the distribution of cutaneous sensory afferent axons. Developmentally, Pbx3 is expressed in a subset of glutamatergic neurons in deeper layers of the dorsal horn that invariably coexpress Meis proteins, a second major family of Hox cofactors. Although the overall balance of GABAergic and glutamatergic neurons is normal in Pbx3C/B1 embryos, we found that the Meis(+) subpopulation was shifted superficially by E15, and that, at this same stage, calbindin(+) cells were overrepresented by approximately three-fold in mutant embryos. Collectively, these results establish that Pbx3 function is required for the specification of a subset of glutamatergic neurons in the dorsal horn, and that its loss results in alterations of dorsal horn lamination and, eventually, postnatal neuron loss. In the absence of marked changes in higher motor centers, the ventral horn, or the dorsal root ganglia, we hypothesize that the cell losses and altered organization of the dorsal horn are sufficient to lead to the observed behavioral abnormalities.

#### *A novel movement disorder in Pbx3C/B1 mutants*

Movement disorders can arise from alterations at a variety of levels of the nervous or musculoskeletal systems involved in the planning, control or execution of movement, and may have multiple causes (Klein, 2005). Our data do not establish that the

behavioral phenotype of Pbx3C/B1 mutants is entirely attributable to changes in the spinal cord, but we did not observe changes in other components of the major systems that govern posture and locomotion. It is also highly unlikely that the phenotype is attributable to alterations of Hoxb1 function, as animals heterozygous for null alleles of Hoxb1 are phenotypically normal, and homozygous mutants do not have abnormal postures or locomotion (Goddard et al., 1996; Studer et al., 1996). In Pbx3C/B1 mutants, the conditional allele was not recombined in the cerebrum, cerebellum or midbrain. It was rendered null in rhombomere 4 of the hindbrain, which is the site of entry of the vestibular nerve and includes some cells of the vestibular nuclei (Guthrie, 1996). The vestibular nuclei did not appear to be altered by the loss of Pbx3 function in r4. Moreover, the mutant mice had vigorous righting reflexes and did not show the abnormal head movements or circling behavior that are often associated with altered vestibular function (Deol, 1956). We and others (Rhee et al., 2004) failed to detect obvious abnormalities in the musculoskeletal or peripheral nervous systems of Pbx3 null mutant embryos at late gestational stages.

The most striking morphological defects we observed in the Pbx3C/B1 mutants were in the superficial layers of the dorsal horn, where clear changes were present by E15. This is in stark contrast to the ventral horn, where we found little evidence of morphological alterations in adult mutants. The overall size of the ventral cord was only slightly decreased, and counts of ventral motor neurons and Renshaw cells in mutants were similar to those obtained in controls. Given that Hox gene

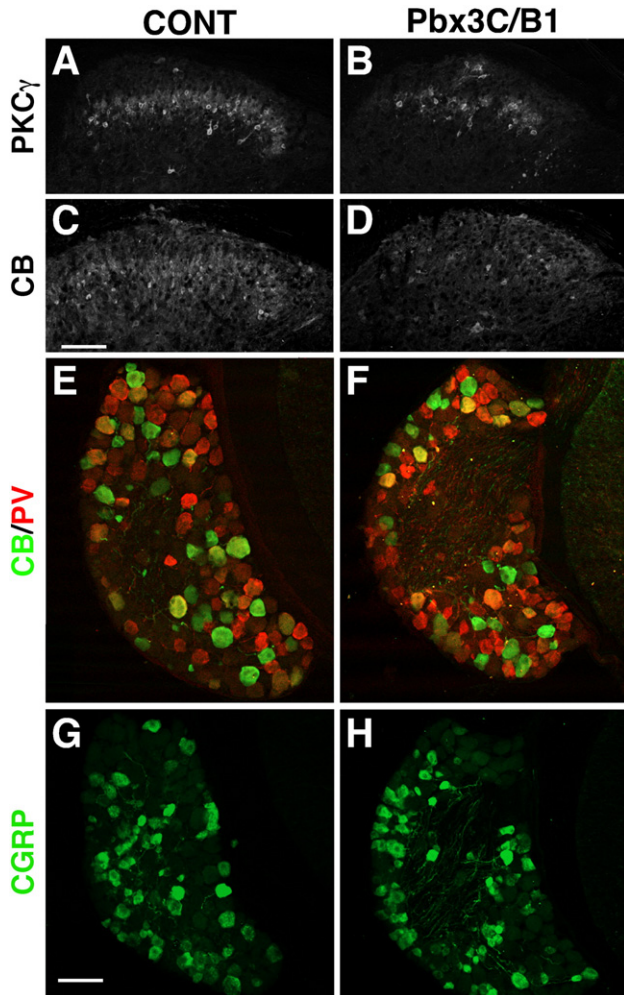


Fig. 10. The DRGs of postnatal day 15 (P15) mutant animals appear normal despite significant disruption of dorsal horn structure. (A–D) Immunohistochemistry of C8 spinal cord of juvenile wild-type (A, C) and Pbx3C/B1 mutant (B, D) mice using antibodies to protein kinase C- $\gamma$  (PKC- $\gamma$ ) (A, B) and calbindin (CB) (C, D). The number and mediolateral continuity of the neurons labeled with the markers appeared altered at this early age as in adult animals. (E–H) Immunohistochemistry of the C8 DRG of P15 control (E, G) and Pbx3C/B1 mutant (F, H) mice using antibodies to calbindin (CB) (E, F), parvalbumin (PV) (E, F) and calcitonin-gene related protein (CGRP) (G, H). The number and distribution of each of these DRG neuronal markers was comparable in mutant and control animals. Scale bars: 100  $\mu$ M.

function is critical to the specification of some to motor neuron classes (Dasen et al., 2003; Dasen et al., 2005), it is likely that Pbx function is also important for the normal development of these neurons. We have found that *Pbx1* mRNA is expressed at high level in many motor neurons of the chick spinal cord (not shown). We speculate that the apparent lack of changes in motor neuron numbers in Pbx3C/B1 mutant mice may be due to largely redundant activities of Pbx1 in this population. We were unable to identify markers for the ventral interneurons that expressed Pbx3 but did not express motor neuron makers, making it impossible to accurately determine if they survived or were altered in the Pbx3C/B1 mutants. It thus remains formally possible that alterations in these cells contribute to the behavioral phenotypes of the mutants.

The superficial laminae of the dorsal horn receive sensory information from cutaneous receptors in the periphery (Fitzgerald, 2005), and the reduced sensitivity of the mutants to thermal and mechanical stimuli are consistent with the substantial losses of superficial neurons observed in the mutants. We think it is important to note the temporal relationship between the changes in the dorsal horn and the changes in the trajectories of cutaneous afferent fibers in Pbx3C/B1 mutants. Alterations in the laminar positions and numbers of specific subsets of glutamatergic neurons are apparent in the spinal cord of E15.5 mutant embryos, before cutaneous fibers invade the neuropil of the dorsal horn. Additionally, the DRGs of mutant animals appeared grossly normal at P15 when severe neuronal losses in the dorsal horn were evident. These data support the suggestion that the changes in dorsal horn structure do not occur in response to changes in the periphery.

It is more difficult to correlate the alterations in posture and locomotion with the superficial neuron losses. The literature suggests that mice can suffer significant loss of cutaneous sensation without developing abnormal postures or locomotion. Adult *Drg11* mutant mice have greatly reduced cutaneous sensation and highly aberrant dorsal horn morphogenesis without developing pronounced deficits of posture or locomotion (Chen et al., 2001). Additionally, overexpression of *Hoxa5* results in severe neuronal loss in the superficial laminae of the dorsal horn at brachial levels and diminished nociception, but locomotion is largely unaffected (Krieger et al., 2004). Unfortunately, mice homozygous for null alleles of a variety of other factors, such as

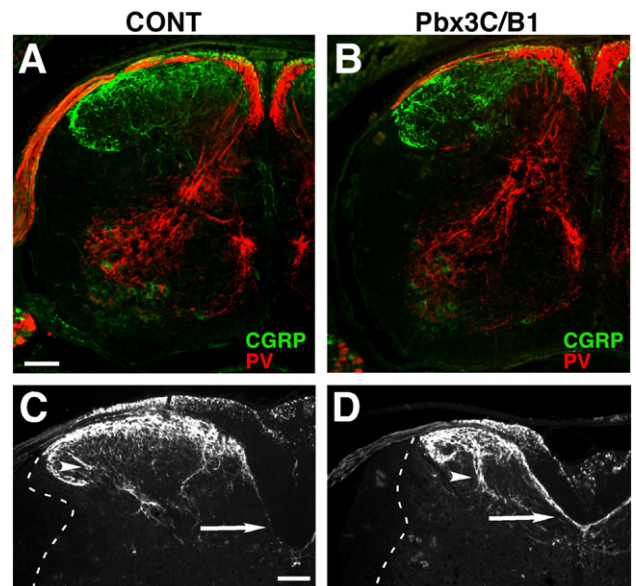


Fig. 11. Alterations of cutaneous sensory afferents in adolescent Pbx3C/B1. (A, B) Sections of control (A) and Pbx3C/B1 (B) brachial spinal cord at P0 labeled with an antibody to CGRP to label cutaneous sensory afferents and parvalbumin (PV) to label proprioceptive afferents. The density and distribution of both types of sensory fibers appear normal in Pbx3C/B1 spinal cords. (C, D) Immunohistochemistry of 2-week-old control (C) and Pbx3C/B1 (D) C8 dorsal spinal cord with antibodies to CGRP. In Pbx3C/B1 mutants abnormally thickened fascicles of CGRP(+) fibers followed normal trajectories adjacent to the dorsal funiculus (arrows) and formed thick cords in more lateral regions of the dorsal horn that were rarely seen in controls (arrowheads). Scale bars: 100  $\mu$ M.

Lbx1, Tlx1/3, Lmx1b, Ptf1a (Cheng et al., 2004; Ding et al., 2004; Glasgow et al., 2005; Gross et al., 2002; Muller et al., 2002), that show grossly abnormal dorsal horn development at midgestational stages do not survive to stages where behavior can be observed.

The abnormal limb postures and locomotion of Pbx3C/B1 mutants resemble mild forms of the postures and ataxia seen in mice with major alterations of proprioceptive neuronal circuitry. These include mice lacking neurotrophin-3, its receptor Ntrk3 (TrkC), or the runt related transcription factor 3 (Runx3) (Ernfors et al., 1994; Inoue et al., 2003; Klein et al., 1994; Levanon et al., 2002). Each of these mutations results in the loss of all or most proprioceptive afferent input to the spinal cord. In Pbx3C/B1 mutants, by contrast, proprioceptive DRG neurons are generated in apparently normal numbers, their survival into adult life suggests that they form appropriate peripheral connections, and the distribution of parvalbumin(+) afferents in the spinal cord is not grossly altered. Thus, if there is a deficit in the integration of proprioceptive sensation into spinal neuron networks controlling movement, it is likely to arise from perturbations of intrinsic spinal cord circuitry.

The displacement of glutamatergic, Meis(+) neurons from deep to superficial positions within the dorsal horn of the mutant mice could potentially lead to alterations in proprioception and locomotion. Mechanoreceptors of a variety of modalities that are integrally involved in the control of movement terminate on interneurons in laminae III and IV (Ralston et al., 1984; Shortland et al., 1989), and these neurons are activated by non-nociceptive afferent input during locomotion (Dai et al., 2005; Jasmin et al., 1994). The input from the periphery is also modified pre-synaptically by the intrinsic oscillation of deep dorsal interneurons (Rossignol et al., 2006). The shift of Meis(+) neurons from deep to superficial positions could affect proprioception by altering the processing of information from mechanoreceptors that normally terminate in laminae III and IV, or by changing the activity of the intrinsic oscillator.

#### *Developmental alterations in Pbx3C/B1 animals*

A major branch point in the differentiation of late-born dorsal horn neurons is the adoption of either a glutamatergic or a GABAergic phenotype. This decision is governed by the activities of the post-mitotic selector genes Tlx1/3 in glutamatergic precursors, and Ptf1a in GABAergic precursors (Cheng et al., 2004; Glasgow et al., 2005). In this context, it is notable that PBC and Meis proteins synergize with Tlx3 to enhance transcription from Tlx3-responsive elements (Rhee et al., 2004). The apparently identical origin of the neonatal apnea observed in Pbx3 and Tlx3 null mutants suggests that this interaction is relevant *in vivo* (Rhee et al., 2004; Shirasawa et al., 2000). Tlx3-dependent neuronal phenotypes in the dorsal horn include a population of early-born neurons that settle in the deep layers (Qian et al., 2001) and a population of late-born neurons that settle superficially (Cheng et al., 2004). Both of these populations were present in Pbx3C/B1 embryos and their numbers were not obviously reduced, despite the fact that Pbx3 is expressed in a subset of each population. It is therefore clear that

Pbx3 function is not uniquely required for the specification of glutamatergic neurotransmitter phenotypes in the dorsal horn. These data do not rule out a role for PBC protein function in the Tlx-dependent specification of neuronal phenotypes, as there is considerable functional redundancy among members of the Pbx family.

Despite the apparently normal balance between glutamatergic and GABAergic markers in mutant embryos, the number of calbindin(+) cells in the dorsal horn was significantly elevated at E15.5. In the mature spinal cord, calbindin expression is primarily associated with excitatory neurons in lamina I and outer lamina II (Antal et al., 1990, 1991; Ren and Ruda, 1994), that include both local circuit and projection neurons that process information of multiple sensory modalities and project locally and to supraspinal levels (Craig et al., 2002). The elevated numbers of calbindin(+) neurons at E15.5 suggests that other neuronal populations may also be perturbed, but many of the markers used to identify these other phenotypes are not expressed embryonically. Unfortunately, by the time these markers were expressed at P15, the gross organization of the dorsal horn was disrupted in the mutant mice.

A second notable change in the dorsal horn morphology at E15.5 was a shift in the positions of Meis(+) glutamatergic neurons to superficial layers of the dorsal horn. In control spinal cords Pbx3 is co-expressed in large proportion of Meis(+) neurons in the deep dorsal horn. This raises the possibility that Pbx3 influences the migration of Meis(+) neurons, thereby affecting their final laminar positions. PBC proteins have been shown to influence neuronal migration of developing cranial motor neurons by both cell autonomous and non-autonomous mechanisms (Cooper et al., 2003). The hypothesis that Pbx3 expression in Meis(+) cells specifies adoption of relatively deep laminar positions through a cell autonomous mechanism can be tested experimentally.

#### *Potential molecular mechanisms of Pbx3 activity in dorsal spinal cord development*

PBC proteins interact with members of the Hox, Engrailed, and Tlx families of transcription factors, all of which are known to influence neural development (Moens and Selleri, 2006). We have commented above on the potential significance of interactions with Tlx proteins in the generation of the Pbx3C/B1 phenotype. It is unlikely that altered Engrailed function contributes to the dorsal horn phenotype because Engrailed proteins are not expressed in the dorsal spinal cord (Davis and Joyner, 1988; Matise and Joyner, 1997). By contrast, Hox proteins are expressed in both the dorsal and ventral spinal cord throughout its length (Dasen et al., 2003). Differences in Hox gene expression establish boundaries between brachial, thoracic and lumbar motor neuron columns (Dasen et al., 2003). Within the brachial and lumbar levels, the differential expression of Hox proteins contributes to the specification of individual motor neuron pools that project to specific peripheral targets (Carpenter et al., 1997; Dasen et al., 2005; de la Cruz et al., 1999; Shah et al., 2004; Wahba et al., 2001). Because PBC proteins are required for many of the functions of Hox proteins from paralogue groups

1–8 (Mann and Chan, 1996; Rauskolb et al., 1993), it is likely that members of the PBC family collaborate with Hox proteins in the specification of motor neuron phenotypes, but this remains to be demonstrated experimentally.

Less is known about potential roles for Hox proteins in the development of the dorsal spinal cord. Several members of the Hoxb complex are expressed at high levels in the dorsal spinal cord of mouse embryos between E12.5 and E15.5, when most of the neurons that populate laminae I–IV become postmitotic and migrate to assume their final positions (Ding et al., 2004; Graham et al., 1991; Vogels et al., 1990) and similar expression is seen in avian embryos (Dasen et al., 2005). Neurological phenotypes have not been described for null mutations of many of these, but mutation of *Hoxb8* leads to deficits in locomotion in adult mice (van den Akker et al., 1999). The neurological basis for this behavior has not been determined. The potential importance of Hox genes in dorsal horn development is also suggested by the finding that the misexpression of *HoxA5* in dorsal horn at brachial levels leads to abnormal differentiation and migration of laminae I–III dorsal neurons (Abbott et al., 2005; Joksimovic et al., 2005; Krieger et al., 2004). This results in severe dorsal horn atrophy and sensory dysfunction in adults.

Our findings represent a significant addition to a growing body of evidence demonstrating that PBC gene activity influences the development and function of neural circuits at multiple levels of the vertebrate CNS. PBC proteins are capable of interacting with several classes of factors that act at early stages of transcriptional cascades regulating the specification of the regional and cellular phenotypes at multiple axial levels. Given potential functional redundancies among PBC family members, unraveling these interactions will require ever more selective alterations of gene activity in a variety of experimental systems.

## Acknowledgments

This work was supported by NIH grant GM56525. We thank Lynn Landmesser, Gary Landreth, Robert Miller, Jerry Silver and Sophia Sundararajan for very helpful discussion of this work, Licia Selleri for providing the *Pbx3* constructs and Thomas Jessell, Thomas Muller, Alexandra Joyner and Samuel Pfaff for generous gifts of antibodies and mouse strains. Thanks to Maryanne Pendergast for help with confocal microscopy. Special thanks to Xiu Yang, Yuefang Zhou, Molly Fuller and Kevin Horn for their consistent support in the laboratory.

## Appendix A. Supplementary data

Supplementary data associated with this article can be found, in the online version, at doi:10.1016/j.ydbio.2007.10.046.

## References

Abbott, M.A., et al., 2005. Ectopic *HOXA5* expression results in abnormal differentiation, migration and p53-independent cell death of superficial dorsal horn neurons. *Brain Res. Dev. Brain Res.* 159, 87–97.

Antal, M., et al., 1990. Calcium-binding proteins, parvalbumin- and calbindin-D

28k-immunoreactive neurons in the rat spinal cord and dorsal root ganglia: a light and electron microscopic study. *J. Comp. Neurol.* 295, 467–484.

Antal, M., et al., 1991. Different populations of parvalbumin- and calbindin-D28k-immunoreactive neurons contain GABA and accumulate 3H-D-aspartate in the dorsal horn of the rat spinal cord. *J. Comp. Neurol.* 314, 114–124.

Arenkiel, B.R., et al., 2003. *Hoxb1* neural crest preferentially form glia of the PNS. *Dev. Dyn.* 227, 379–386.

Berthelsen, J., et al., 1998. The novel homeoprotein *Prep1* modulates *Pbx*–Hox protein cooperativity. *EMBO J.* 17, 1434–1445.

Berthelsen, J., et al., 1999. The subcellular localization of *PBX1* and *EXD* proteins depends on nuclear import and export signals and is modulated by association with *PREP1* and *HTH*. *Genes Dev.* 13, 946–953.

Bradbury, E.J., et al., 2002. Chondroitinase ABC promotes functional recovery after spinal cord injury. *Nature* 416, 636–640.

Brendolan, A., et al., 2005. A *Pbx1*-dependent genetic and transcriptional network regulates spleen ontogeny. *Development* 132, 3113–3126.

Capellini, T.D., et al., 2006. *Pbx1/Pbx2* requirement for distal limb patterning is mediated by the hierarchical control of Hox gene spatial distribution and *Shh* expression. *Development* 133, 2263–2273.

Carpenter, E.M., et al., 1997. Targeted disruption of *Hoxd-10* affects mouse hindlimb development. *Development* 124, 4505–4514.

Caspary, T., Anderson, K.V., 2003. Patterning cell types in the dorsal spinal cord: what the mouse mutants say. *Nat. Rev., Neurosci.* 4, 289–297.

Chaplan, S.R., et al., 1994. Quantitative assessment of tactile allodynia in the rat paw. *J. Neurosci. Methods* 53, 55–63.

Chen, Z.F., et al., 2001. The paired homeodomain protein *DRG11* is required for the projection of cutaneous sensory afferent fibers to the dorsal spinal cord. *Neuron* 31, 59–73.

Chen, A.I., et al., 2006. Graded activity of transcription factor *Runx3* specifies the laminar termination pattern of sensory axons in the developing spinal cord. *Neuron* 49, 395–408.

Cheng, L., et al., 2004. *Tlx3* and *Tlx1* are post-mitotic selector genes determining glutamatergic over GABAergic cell fates. *Nat. Neurosci.* 7, 510–517.

Cooper, K.L., et al., 2003. Autonomous and nonautonomous functions for *Hox/Pbx* in branchiomotor neuron development. *Dev. Biol.* 253, 200–213.

Craig, A.D., et al., 2002. Association of spinothalamic lamina I neurons and their ascending axons with calbindin-immunoreactivity in monkey and human. *Pain* 97, 105–115.

Dai, X., et al., 2005. Localization of spinal neurons activated during locomotion using the *c-fos* immunohistochemical method. *J. Neurophysiol.* 93, 3442–3452.

Dasen, J.S., et al., 2003. Motor neuron columnar fate imposed by sequential phases of *Hox-c* activity. *Nature* 425, 926–933.

Dasen, J.S., et al., 2005. A Hox regulatory network establishes motor neuron pool identity and target–muscle connectivity. *Cell* 123, 477–491.

Davis, C.A., Joyner, A.L., 1988. Expression patterns of the homeo box-containing genes *En-1* and *En-2* and the proto-oncogene *int-1* diverge during mouse development. *Genes Dev.* 2, 1736–1744.

Dear, T.N., et al., 1995. The *Hox11* gene is essential for cell survival during spleen development. *Development* 121, 2909–2915.

de la Cruz, C.C., et al., 1999. Targeted disruption of *Hoxd9* and *Hoxd10* alters locomotor behavior, vertebral identity, and peripheral nervous system development. *Dev. Biol.* 216, 595–610.

Deol, M.S., 1956. The anatomy and development of the mutants *pirouette*, *shaker-1* and *waltzer* in the mouse. *Proc. R. Soc. Lond., B Biol. Sci.* 145, 206–213.

Di Giacomo, G., et al., 2006. Spatio-temporal expression of *Pbx3* during mouse organogenesis. *Gene Expr. Patterns* 6, 747–757.

Ding, Y.Q., et al., 2004. *Lmx1b* controls the differentiation and migration of the superficial dorsal horn neurons of the spinal cord. *Development* 131, 3693–3703.

Erickson, T., et al., 2007. *Pbx* proteins cooperate with *Engrailed* to pattern the midbrain–hindbrain and diencephalic–mesencephalic boundaries. *Dev. Biol.* 301, 504–517.

Ernfors, P., et al., 1994. Lack of neurotrophin-3 leads to deficiencies in the peripheral nervous system and loss of limb proprioceptive afferents. *Cell* 77, 503–512.

- Ferretti, E., et al., 2005. Hoxb1 enhancer and control of rhombomere 4 expression: complex interplay between PREP1–PBX1–HOXB1 binding sites. *Mol. Cell. Biol.* 25, 8541–8552.
- Fitzgerald, M., 2005. The development of nociceptive circuits. *Nat. Rev., Neurosci.* 6, 507–520.
- Frohman, M.A., et al., 1990. Isolation of the mouse Hox-2.9 gene; analysis of embryonic expression suggests that positional information along the anterior–posterior axis is specified by mesoderm. *Development* 110, 589–607.
- Gaufo, G.O., et al., 2004. Contribution of Hox genes to the diversity of the hindbrain sensory system. *Development* 131, 1259–1266.
- Glasgow, S.M., et al., 2005. Ptf1a determines GABAergic over glutamatergic neuronal cell fate in the spinal cord dorsal horn. *Development* 132, 5461–5469.
- Goddard, J.M., et al., 1996. Mice with targeted disruption of Hoxb-1 fail to form the motor nucleus of the VIIth nerve. *Development* 122, 3217–3228.
- Graham, A., et al., 1991. The murine Hox-2 genes display dynamic dorsoventral patterns of expression during central nervous system development. *Development* 112, 255–264.
- Gross, M.K., et al., 2002. Lbx1 specifies somatosensory association interneurons in the dorsal spinal cord. *Neuron* 34, 535–549.
- Guthrie, S., 1996. Patterning the hindbrain. *Curr. Opin. Neurobiol.* 6, 41–48.
- Hasty, P., et al., 1991. Introduction of a subtle mutation into the Hox-2.6 locus in embryonic stem cells. *Nature* 350, 243–246.
- Inoue, K., et al., 2003. Runx3 is essential for the target-specific axon pathfinding of trkc-expressing dorsal root ganglion neurons. *Blood Cells Mol. Diseases* 30, 157–160.
- Jacobs, Y., et al., 1999. Trimeric association of Hox and TALE homeodomain proteins mediates Hoxb2 hindbrain enhancer activity. *Mol. Cell. Biol.* 19, 5134–5142.
- Jasmin, L., et al., 1994. Walking evokes a distinctive pattern of Fos-like immunoreactivity in the caudal brainstem and spinal cord of the rat. *Neuroscience* 58, 275–286.
- Joksimovic, M., et al., 2005. Dynamic expression of murine HOXA5 protein in the central nervous system. *Gene Expr. Patterns* 5, 792–800.
- Klein, C., 2005. Movement disorders: classifications. *J. Inherit. Metab. Dis.* 28, 425–439.
- Klein, R., et al., 1994. Disruption of the neurotrophin-3 receptor gene trkC eliminates la muscle afferents and results in abnormal movements. *Nature* 368, 249–251.
- Kobayashi, M., et al., 2003. Engrailed cooperates with extradenticle and homothorax to repress target genes in Drosophila. *Development* 130, 741–751.
- Krieger, K.E., et al., 2004. Transgenic mice ectopically expressing HOXA5 in the dorsal spinal cord show structural defects of the cervical spinal cord along with sensory and motor defects of the forelimb. *Brain Res. Dev. Brain Res.* 150, 125–139.
- Lee, S.K., Pfaff, S.L., 2001. Transcriptional networks regulating neuronal identity in the developing spinal cord. *Nat. Neurosci.* 4, 1183–1191.
- Levanon, D., et al., 2002. The Runx3 transcription factor regulates development and survival of TrkC dorsal root ganglia neurons. *EMBO J.* 21, 3454–3463.
- Mann, R.S., Chan, S.K., 1996. Extra specificity from extradenticle: the partnership between HOX and PBX/EXD homeodomain proteins. *Trends Genet.* 12, 258–262.
- Matise, M.P., Joyner, A.L., 1997. Expression patterns of developmental control genes in normal and Engrailed-1 mutant mouse spinal cord reveal early diversity in developing interneurons. *J. Neurosci.* 17, 7805–7816.
- Mizuguchi, R., et al., 2006. Ascl1 and Gsh1/2 control inhibitory and excitatory cell fate in spinal sensory interneurons. *Nat. Neurosci.* 9, 770–778.
- Moens, C.B., Selleri, L., 2006. Hox cofactors in vertebrate development. *Dev. Biol.* 291, 193–206.
- Monica, K., et al., 1991. PBX2 and PBX3, new homeobox genes with extensive homology to the human proto-oncogene PBX1. *Mol. Cell. Biol.* 11, 6149–6157.
- Muller, T., et al., 2002. The homeodomain factor Lbx1 distinguishes two major programs of neuronal differentiation in the dorsal spinal cord. *Neuron* 34, 551–562.
- Murphy, P., et al., 1989. Segment-specific expression of a homeobox-containing gene in the mouse hindbrain. *Nature* 341, 156–159.
- O’Gorman, S., 2005. Second branchial arch lineages of the middle ear of wild-type and Hoxa2 mutant mice. *Dev. Dyn.* 234, 124–131.
- O’Gorman, S., et al., 1997. Protamine-Cre recombinase transgenes efficiently recombine target sequences in the male germ line of mice, but not in embryonic stem cells. *Proc. Natl. Acad. Sci. U. S. A.* 94, 14602–14607.
- Peifer, M., Wieschaus, E., 1990. Mutations in the Drosophila gene extradenticle affect the way specific homeo domain proteins regulate segmental identity. *Genes Dev.* 4, 1209–1223.
- Pillai, A., et al., 2007. Lhx1 and Lhx5 maintain the inhibitory-neurotransmitter status of interneurons in the dorsal spinal cord. *Development* 134, 357–366.
- Pinsonneault, J., et al., 1997. A model for extradenticle function as a switch that changes HOX proteins from repressors to activators. *EMBO J.* 16, 2032–2042.
- Qian, Y., et al., 2001. Formation of brainstem (nor)adrenergic centers and first-order relay visceral sensory neurons is dependent on homeodomain protein Rnx/Tlx3. *Genes Dev.* 15, 2533–2545.
- Ralston III, H.J., et al., 1984. Morphology and synaptic relationships of physiologically identified low-threshold dorsal root axons stained with intraxonal horseradish peroxidase in the cat and monkey. *J. Neurophysiol.* 51, 777–792.
- Rauskolb, C., et al., 1993. Extradenticle, a regulator of homeotic gene activity, is a homolog of the homeobox-containing human proto-oncogene pbx1. *Cell* 74, 1101–1112.
- Ren, K., Ruda, M.A., 1994. A comparative study of the calcium-binding proteins calbindin-D28K, calretinin, calmodulin and parvalbumin in the rat spinal cord. *Brain Res. Brain Res. Rev.* 19, 163–179.
- Rhee, J.W., et al., 2004. Pbx3 deficiency results in central hypoventilation. *Am. J. Pathol.* 165, 1343–1350.
- Rijli, F.M., et al., 1993. A homeotic transformation is generated in the rostral branchial region of the head by disruption of Hoxa-2, which acts as a selector gene. *Cell* 75, 1333–1349.
- Roberts, C.W., et al., 1994. Hox11 controls the genesis of the spleen. *Nature* 368, 747–749.
- Roberts, V.J., et al., 1995. Localization of Pbx1 transcripts in developing rat embryos. *Mech. Dev.* 51, 193–198.
- Rossignol, S., et al., 2006. Dynamic sensorimotor interactions in locomotion. *Physiol. Rev.* 86, 89–154.
- Ryoo, H.D., et al., 1999. Regulation of Hox target genes by a DNA bound Homothorax/Hox/Extradenticle complex. *Development* 126, 5137–5148.
- Saleh, M., et al., 2000. Cell signaling switches HOX–PBX complexes from repressors to activators of transcription mediated by histone deacetylases and histone acetyltransferases. *Mol. Cell. Biol.* 20, 8623–8633.
- Schaeren-Wiemers, N., Gerfin-Moser, A., 1993. A single protocol to detect transcripts of various types and expression levels in neural tissue and cultured cells: in situ hybridization using digoxigenin-labelled cRNA probes. *Histochemistry* 100, 431–440.
- Selleri, L., et al., 2001. Requirement for Pbx1 in skeletal patterning and programming chondrocyte proliferation and differentiation. *Development* 128, 3543–3557.
- Selleri, L., et al., 2004. The TALE homeodomain protein Pbx2 is not essential for development and long-term survival. *Mol. Cell. Biol.* 24, 5324–5331.
- Shah, V., et al., 2004. Ectopic expression of Hoxd10 in thoracic spinal segments induces motoneurons with a lumbosacral molecular profile and axon projections to the limb. *Dev. Dyn.* 231, 43–56.
- Shirasawa, S., et al., 2000. Rnx deficiency results in congenital central hypoventilation. *Nat. Genet.* 24, 287–290.
- Shortland, P., et al., 1989. Morphology and somatotopic organization of the central terminals of hindlimb hair follicle afferents in the rat lumbar spinal cord. *J. Comp. Neurol.* 289, 416–433.
- Soriano, P., 1999. Generalized lacZ expression with the ROSA26 Cre reporter strain. *Nat. Genet.* 21, 70–71.
- Studer, M., et al., 1996. Altered segmental identity and abnormal migration of motor neurons in mice lacking Hoxb-1. *Nature* 384, 630–634.
- Thallmair, M., et al., 1998. Neurite growth inhibitors restrict plasticity and functional recovery following corticospinal tract lesions. *Nat. Neurosci.* 1, 124–131.
- Thomas, K.R., Capecchi, M.R., 1986. Introduction of homologous DNA

- sequences into mammalian cells induces mutations in the cognate gene. *Nature* 324, 34–38.
- Tybulewicz, V.L., et al., 1991. Neonatal lethality and lymphopenia in mice with a homozygous disruption of the *c-abl* proto-oncogene. *Cell* 65, 1153–1163.
- van den Akker, E., et al., 1999. Targeted inactivation of *Hoxb8* affects survival of a spinal ganglion and causes aberrant limb reflexes. *Mech. Dev.* 89, 103–114.
- Vogels, R., et al., 1990. Expression of the murine homeobox-containing gene *Hox-2.3* suggests multiple time-dependent and tissue-specific roles during development. *Development* 110, 1159–1168.
- Wahba, G.M., et al., 2001. The paralogous *Hox* genes *Hoxa10* and *Hoxd10* interact to pattern the mouse hindlimb peripheral nervous system and skeleton. *Dev. Biol.* 231, 87–102.
- Waskiewicz, A.J., et al., 2001. Zebrafish *Meis* functions to stabilize *Pbx* proteins and regulate hindbrain patterning. *Development* 128, 4139–4151.